# Anti-cancer effects of aqueous extracts of *Dodonaea viscosa* on Burkitt lymphoma

**Aaliyah Saferdien**




Thesis presented for the Degree of

**DOCTOR OF PHILOSOPHY**

*In the Division of Haematology*

*Department of Pathology*

*Faculty of Health Sciences*

*University of Cape Town*

Supervisor: A/Prof Shaheen Mowla

September 2023

# Declaration

I, Aaliyah Saferdien, hereby declare that the work on which this Doctoral thesis is based is my original work (except where acknowledgements indicate otherwise) and that neither the whole work nor any part of it has been, is being, or is to be submitted for another degree in this or any other University.

I empower the University to reproduce for the purpose of research either the whole or any portion of the contents in any manner whatsoever.

Signature_____

September 2023

# Acknowledgments

Reflecting on this past year, completing this thesis has been my most formidable challenge. It began with excitement and disbelief that the time had finally come to embark on this journey. I set forth with great anticipation and unwavering focus. However, as weeks turned into months, I encountered unexpected obstacles. It demanded more time, more revisions, and more research than I had initially anticipated. Yet, throughout this arduous journey, the love and support of my family and the camaraderie of my colleagues provided me with the perspective and resilience to persevere. I would like to express my heartfelt gratitude to the pillars in my life who have made this moment possible and have been with me throughout this journey.

I would like to begin by praising and thanking my creator, Allah (SWT) for granting me this opportunity to complete my Ph.D. and blessing me with good health, strength, and the ability to pursue my dreams. I recognize the privilege of the opportunities I have been granted, and I am humbled by the abundance of blessings in my life.

To my parents, siblings, and extended family, your unwavering support and encouragement have been my guiding light throughout this journey. You have instilled in me the belief that I can achieve anything I set my mind to, and for that, I am eternally grateful.

Next, I would like to express my gratitude to my fellow scientists and lab rats Lungile, Leo, Beatrice, Babalwa, Zahra, Marian, Thando and Lincoln. Thank you for all your kind-heartedness, memories, laughs and making the long tiring days of lab work bearable. To the Division of Haematology staff, A/Prof Jessica Opie, A/Prof Karen Shires, Jolene, Cylene, Zhaheed and ex-staff members (Jean, Rygana and Colleen) thank you for your support, assistance, academic and life advice over these last few years.

Thank you to Rodney Lucas for his assistance and training on the *in vivo* work and to A/Prof Glenda Davidson and Ronnie Dreyer for their assistance and training on the flow cytometer.

I would like to also express my sincere gratitude to the following funders: South African Medical Research Council – Bongani Mayosi National Health Scholars Programme, the National Research Foundation, University of Cape Town, and the Fogarty International Centre of the National Institutes of Health – Fogarty Research Training Program.

Lastly, I would like to give a special thank you to my supervisor, A/Prof Shaheen Mowla. Thank you for all the support, patience, mentorship, knowledge, and kindness over the last 7 years. I started out as a naïve honours student in your lab and through your guidance and mentoring, I am able to complete this doctoral degree. Words cannot describe how grateful I am to have had you as a supervisor, mentor, and friend over the last few years.

Today, as I stand at the culmination of this endeavour, I am filled with a profound sense of accomplishment. This thesis represents not just a piece of academic work, but a testament to the strength of my character and the incredible support system that surrounds me.

In closing, I extend my gratitude to everyone who played a role, however big or small, in this accomplishment. Your belief in me has been the wind beneath my wings, propelling me forward even in the face of challenges. I hope to continue to make you proud as I embark on the next chapter of my journey.

# Table of Contents

# List of Figures

# List of Tables

# Abbreviations

| | |
|---|---|
| 7-AAD | 7-Amino-Actinomycin |
| AEC | Animal Research Ethics Committee |
| AIDS | Acquired Immunodeficiency Syndrome |
| ANOVA | Analysis of Variance |
| ART | Antiretroviral therapy |
| ATCC | American Type Culture Collection |
| BCA | Bicinchonic acid |
| BCR | B Cell Receptor |
| BL | Burkitt Lymphoma |
| BSA | Bovine Serum Albumin |
| CAM | Complementary and Alternative Medicine |
| CANSA | The Cancer Association of South Africa |
| CCND3 | Cyclin D3 |
| CD | Cell debris |
| CFSE | Carboxyfluorescein Succinimidyl Ester |
| $CO_2$ | Carbon Dioxide |
| COP | Cyclophosphamide, Vincristine, Prednisone |
| CODOX-M/IVAC | Cyclophosphamide, Doxorubicin, Vincristine, high-dose Methotrexate/ Ifosfamide, high-dose Cytarabine, and Etoposide |
| COPADM/CYVE | Cyclophosphamide, Vincristine, Prednisone, Doxorubicin, Methotrexate, Cytarabine, Etoposide |
| CS | Cell Swelling |
| DLBCL | Diffused Large B Cell Lymphoma |
| DNA | Deoxyribonucleic acid |
| DMEM | Dulbecco's Modified Eagles Medium |
| DMSO | Dimethyl Sulfoxide |
| DoH | South African National Department of Health |
| DOX | Doxorubicin |
| DTT | Dithiothreitol |
| DV | *Dodonaea viscosa* |

| | |
|---|---|
| DVE | *Dodonaea viscosa* Extract |
| EDTA | Ethylenediaminetetraacetic acid |
| FBS | Fetal Bovine Serum |
| FDA | Food and Drug Administration |
| GPCR | G-protein coupled receptor |
| GSK3 | Glycogen Synthase Kinase 3 |
| HCL | Hydrochloride |
| HIV | Human Immunodeficiency Virus |
| HRP | Horseradish peroxidase |
| Hyper-CVAD | Hyper-fractionated Cyclophosphamide, Vincristine, Doxorubicin, Dexamethasone, Methotrexate, Cytarabine |
| IARC | International Agency for Research on Cancer |
| ID3 | Inhibitor of DNA Binding 3 |
| IGH | Immunoglobulin Heavy Chain |
| LCL | Lymphoblastoid Cell Line |
| MAPK | Mitogen-Activated Protein Kinases |
| MB | Membrane Blebbing |
| MDR | Multi-Drug Resistance |
| mTORC2 | Mammalian Target of Rapamycin Complex 2 |
| ND | Nuclear Dissolution |
| NOD SCID | Non Obese Diabetic Severe Combined Immunodeficiency |
| NHL | Non-Hodgkin Lymphoma |
| NSCLC | Non-Small Cell Lung Cancer |
| OS | Overall Survival |
| P1 | Parent cell generation |
| P2 | Daughter cell generation |
| PA | Phosphatidic acid |
| PAGE | Polyacrylamide Gel Electrophoresis |
| PARP-1 | Poly ADP-ribose Polymerase |
| PBS | Phosphate Buffered Saline |
| PC | Phosphatidylcholine |

| | |
|---|---|
| PDK-1 | Phosphoinositide Dependent Kinase 1 |
| PE | Phycoerythrin |
| PE | Phosphatidylethanolamine |
| PS | Phosphatidylserine |
| PI3K | Phosphatidylinositol 3-kinase |
| PIP2 | Phosphatidylinositol-4,5-bisphosphate |
| PIP3 | Phosphatidylinositol-3,4,5-triphosphate |
| PLWHA | People living with HIV/AIDS |
| P/S | Penicillin/Streptomycin |
| PTEN | Phosphatase and Tensin Homolog |
| RPM | Revolutions per minute |
| RPMI | Roswell Park Memorial Institute |
| RTK | Receptor Tyrosine Kinases |
| SA | South Africa |
| SAHPRA | South African Health Products Regulatory Authority |
| SDS | Sodium Dodecyl Sulphate |
| Ser | Serine |
| SI | Selectivity Index |
| SM | Sphingomyelin |
| TBS | Tris-buffered saline |
| TCF3 | Transcription Factor 3 |
| THP | Traditional Health Practitioner |
| Thr | Threonine |
| TLR | Toll-like receptor |
| TMP | Traditional Medical Practitioner |
| UT | Untreated |
| WHO | World Health Organization |

# Abstract

Cancer is a leading public health problem worldwide, and although modern treatments have undeniably improved patient outcomes, many cancers remain refractory or untreatable. New and more effective treatments are needed, and natural phytochemical compounds are a valuable source for the development of such treatments. In South Africa, the high HIV prevalence is a compounding factor in cancer incidence, with some cancers being disproportionately high among HIV-positive individuals. One such cancer is Burkitt lymphoma (BL), a highly aggressive B-cell-derived malignancy, which develops predominantly in HIV-infected individuals. Many cancer patients, especially those from rural communities, use traditional medicine (TM) as an alternative to chemotherapy. While conventional treatments have been thoroughly researched and tested before clinical approval, alternative treatments have not. Therefore, TM may not necessarily be beneficial to patients, could interfere with conventional treatment if used concurrently, and in some instances, be harmful to users.

One TM commonly used by communities in the Western Cape regions of South Africa is derived from the plant *Dodonaea viscosa*. Extracts from this plant have not been widely investigated scientifically, however, preliminary work indicates that it holds potential anti-cancer properties. In the current research, the inhibitory potential of *D. viscosa* extracts (DVE) on BL was comprehensively assessed, using *in vitro* assays, as well as using an *in vivo* mouse model.

Using cell viability assays, the IC50 of DVE on two BL cell lines, namely Ramos and BL41, was determined. The Ramos IC50 was 0.06 mg/ml while that of BL41 was 0.18 mg/ml. Notably, the non-cancerous lymphoblastoid control cell line (LCL) was significantly less sensitive to DVE compared to both BL cell lines with selectivity indices of 2.8 (using IC50) and 1.7 (using IC30) for Ramos and BL41 respectively. Cell Trace proliferation and colony formation assays showed retardation in the proliferation of extract-treated BL cells (3.2-fold and 10.9-fold reduction in progress to daughter cell generation relative to untreated for Ramos and BL41 respectively). Additionally, DVE induced significant apoptosis, as shown by cellular morphological analyses, Annexin V and caspase 3/7 activity assays, cell cycle profiling and western blotting, showing enhanced expression of effector apoptotic markers (cleaved caspase 3 and cleaved PARP). The PI3K/Akt pathway, which is often altered in BL and known to drive lymphomagenesis, was found to mediate, at least partially, the cytotoxicity of DVE – the PI3K inhibitor p-PTEN was upregulated, leading to upregulation of its target p-PDK1. Additionally, the effector molecule p-AKT (ser 473) and p-GSK3$\beta$ were altered. Lastly, using a BL xenograft mouse model, DVE was found to be significantly less toxic than the approved drug Doxorubicin, and to slow down tumour growth over time.

This study revealed that aqueous extracts from the *Dodonaea viscosa* plant, used by traditional healers, is a valuable source of lead compounds for the development of novel therapeutics in the treatment of Burkitt lymphoma.

# Chapter 1: Background and Literature Review

## *1.1 Introduction*

Cancer is one of the leading causes of premature death worldwide. In 2020, the International Agency for Research on Cancer (IARC) analysed the burden of cancer globally and estimated that there were 10 million deaths and 19.3 million new cancer cases (Sung et al., 2021). Further analysis of the incidence and mortality rates revealed that, in contrast to other regions of the world, Africa and Asia have the highest mortality rate with a comparably much lower incidence rate. It is suggested that this is due to the high burden of diseases present in these regions, poor access to quality health care, the availability of treatment regimens, and the presence of infection and poverty-related cancers which are more prevalent in developing regions (Bray et al., 2018; Sung et al., 2021; Torre et al., 2015). This therefore speaks to the need for the development of strategies for cancer management which are targeted to and suited for developing countries.

## *1.2 HIV-associated Lymphoma*

In Southern Africa, a compounding factor to the cancer burden is the high incidence of HIV infection. An estimated 13.7% of the South African population is currently infected with HIV, and since the rollout of the antiretroviral therapy program (ART) in 2004, the lifespan of people living with HIV/AIDS (PLWHA) has increased significantly (Barnabas et al., 2020; Carmona et al., 2018; Statistics South Africa, 2022; Ugwu and Ncayiyana, 2022). Concomitant with this is an increased incidence of HIV-associated cancers within this population group. These include aggressive B-cell derived lymphomas, with Burkitt lymphoma (BL) being one of the most prevalent (Abayomi et al., 2011; Opie et al., 2020).

BL is a type of Non-Hodgkin lymphoma (NHL), a group of blood cancers that develop from B and T lymphocytes and are generally over-represented in the South African population, compared to elsewhere in the world, due to their association with HIV infection. Data from The Cancer Association of South Africa (CANSA) 2019 factsheet shows that Non-Hodgkin lymphoma is among the top ten cancers in both males and females in South Africa. Figure 1.1 below is from a retrospective study conducted at the University of Cape Town where bone marrow biopsy reports of 1215 lymphoma patients diagnosed between 1 January 2005 and 31 December 2010 at Groote Schuur hospital were analysed. It shows the distribution of NHL subtypes by HIV status, showing a six-fold increase in BL diagnosis among HIV infected individuals compared to HIV uninfected ones (Phillips and Opie, 2017).

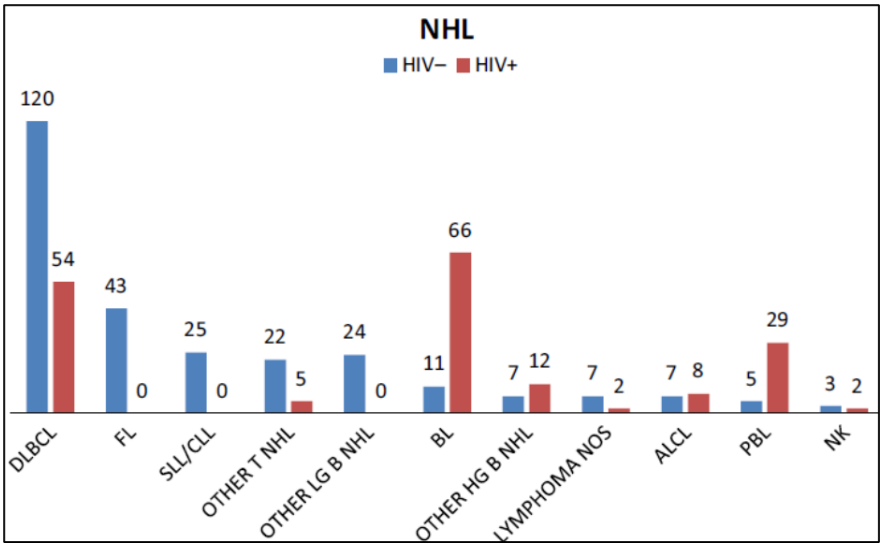


**Figure 1.1: Distribution of Non-Hodgkin lymphoma subtypes by HIV status.** A retrospective study conducted at the University of Cape Town where bone marrow biopsy reports of 1215 lymphoma patients diagnosed between 1 January 2005 and 31 December 2010 at Groote Schuur hospital were analyzed. Reported in Phillips and Opie, (2017)

### *1.3 Burkitt Lymphoma*

Burkitt Lymphoma is an aggressive B cell lymphoma arising from germinal centre B cells that occurs in adults and children. BL is characterised histologically by monomorphic B cells with compact nuclei and many large, irregularly shaped macrophages that are interspersed among the B lymphocytes to give a 'starry sky' appearance (Crombie and LaCasce, 2021). A genetic hallmark of this cancer is translocations of the *MYC* oncogene, with the t(8;14) (q24; q32) rearrangement on the immunoglobulin heavy chain (IGH) being the most common. This rearrangement results in the constitutive overexpression of *MYC*, a potent promoter of proliferation (Crombie and LaCasce, 2021; Zayac and Olszewski., 2020). Gene expression profiling studies have shown that, in addition to the translocation events, other genetic mutations and chromosomal aberrations, particularly those affecting the cyclin-dependent kinase pathways and phosphatidylinositol 3-kinase (PI3K) signalling, also contribute to the oncogenic phenotype (Crombie and LaCasce, 2021; Zayac and Olszewski, 2020).

The PI3K (phosphatidylinositol 3-kinase) pathway is essential for the regulation of cellular proliferation, growth, and apoptosis. Activation of the PI3K pathway in BL is mainly a result of constitutive 'tonic' B-cell receptor (BCR) signalling, characterized by mutations in the TCF3/ID3/CCND3 pathway, seen in up to 70% of BL patients (Rohde et al., 2017; Sander et al., 2012; Schmitz et al., 2012; Schmitz et al., 2014). The transcription factor 3 (TCF3) is constitutively expressed during B-cell development. Mutations in TCF3 or its negative regulator, ID3, causes increased expression of B-cell receptor signalling resulting in continuous activation of the PI3K pathway and increased cellular proliferation, and survival.

Recurrent mutations are also found in Cyclin D3 (CCND3), a direct target of TCF3, in 30% of BL and prevents cell cycle progression at the G1-S phase transition (Crombie and LaCasce, 2021; Dunleavy et al., 2016; Rohde et al., 2017; Schmits et al., 2014; Zayac and Olszewski, 2020).

BL is classified into three different subtypes: (1) Endemic BL, which is predominantly found along the malarial belt and primarily affects children; (2) Sporadic BL which occurs worldwide and accounts for 1% to 2% of adult lymphoma cases, and (3) immunodeficiency-associated BL which is most common among HIV infected patients. Reports indicate that up to 40% of HIV-positive patients develop BL, despite being on anti-retroviral therapy (ART) (Atallah-Yunes et al., 2020; Dunleavy et al., 2020; Hämmerl et al., 2019; Opie et al., 2020). HIV-positive patients with BL typically present with leukaemic dissemination, complex karyotypes, advanced-stage disease, and a high tumour burden, which requires them to receive dose intensive chemotherapy and supportive care. This often results in toxic side effects and other complications (Kalisz et al., 2019; Opie et al., 2020; Turro et al., 2019; Wang et al., 2022). In South Africa, patients are typically initially treated with COP (cyclophosphamide, vincristine, prednisone) and thereafter receive intensive chemotherapeutic regimens including CODOX-M/IVAC (cyclophosphamide, doxorubicin, vincristine, high-dose methotrexate/ ifosfamide, high-dose cytarabine, and etoposide), Hyper-CVAD (hyper-fractionated cyclophosphamide, vincristine, doxorubicin, dexamethasone, methotrexate, cytarabine) and COPADM/CYVE (cyclophosphamide, vincristine, prednisone, doxorubicin, methotrexate, cytarabine, etoposide) (Crombie and LaCasce, 2021; Zayac and Olszewski, 2020)). HIV-infected patients receive ART throughout chemotherapy and in well-resourced settings, will receive rituximab (chimeric anti-CD20 monoclonal immunotherapy) in combination with chemotherapy (Atallah-Yunes et al., 2020; Opie et al., 2020).

One of the greatest challenges of cancer therapy, including BL therapy, is toxicity. Older and immunocompromised patients are particularly at risk of chemotoxicity, leading to poor outcome in these patients. In low-resourced settings, inferior patient outcomes are compounded by limited access to healthcare providers, which in turn leads to inconsistent ART therapy, as well as inequitable access to treatment in public health care facilities (Atallah-Yunes et al., 2020; Dunleavy et al., 2020; Opie et al., 2020). There is therefore a great need not only to improve current BL treatment regimens but also to identify novel drugs which are accessible and affordable to the relevant patient groups. In many communities around the world, complementary and alternative medicine (CAM) is being used by cancer patients to alleviate the side effects of cancer therapy. Importantly, many studies have explored the anti-cancer properties of CAM products as a source for new drugs and the safe use of these drugs in humans (Keene et al., 2019; Knecht et al., 2019; Majolo et al., 2019).

### *1.4 The use of Complementary and Alternative Medicine in South Africa*

In South Africa, where there is an estimated 68 000 (full-time only) to 300 000 (combination of full-time and part-time) practicing Traditional Medical Practitioners, the use of Complementary and Alternative Medicine (CAM) is prevalent (Street et al., 2018). Traditional Medical Practitioners (TMPs) are important providers of alternative treatments to their communities and the role that they play in healthcare provision cannot be overlooked. Many communities rely on TMPs for their primary healthcare needs. Due to their important cultural role, availability, and accessibility, traditional healers are therefore a vital part of health care provision in South Africa. For this reason, various models are being considered and developed, where TMPs can be incorporated into the national healthcare delivery system (Moshabela et al., 2015; Mothibe and Sibanda, 2016; Pinkoane et al., 2012; Street et al., 2018). In 2007 the South African National Department of Health (DoH) developed the Traditional Health Practitioners Act 22 in order to institutionalise and regulate TMP's in South Africa. This act aims to: 1) Create an interim traditional health practitioners' council; 2) provide a regulatory framework to ensure the efficacy, safety, and quality of traditional healthcare services and 3) Manage and control the registration, training, and conduct of practitioners and students in the THP profession (R. A Street, 2016). In accordance with Act 22, the Traditional Health Practitioners council was inaugurated in 2013 and aims to oversee the registration and regulations of TMP's in SA (Moshabela et al., 2015; De Roubaix, 2016). However, South Africa still has a long way to go in developing a model that successfully integrates TMP's into the health care sector which can allow them to be recognised as health professionals with appropriate training, able to provide quality and affordable health care to their patients (M. de Roubaix, 2016; Street et al., 2018).

Regardless, many cancer sufferers continue to use Complementary and Alternative medicine (CAM), mainly for the purpose of combatting the side effects associated with conventional therapies, or to boost their immune system, hoping for an improved quality of life. Some cancer patients choose to use alternative medicine as their main form of treatment instead of the conventional treatment options available to them (Eng et al., 2003; Yates et al., 2005). In developing countries in particular, many cancer patients primarily use CAM as it aligns with their cultural practice, is easily accessible, and is more affordable. WHO estimates show that in many developing countries more than 80% of the population depend on Complementary and Alternative medicine as their primary health care (Oyebode et al., 2016; Yuan et al., 2016).

CAM therapies, unlike conventional western medicine, are not regulated or controlled by any governmental health agency such as the FDA (Food and Drug Administration) in the United States, or the South African Health Products Regulatory Authority (SAHPRA) in South Africa. While conventional

treatments are rigorously researched and tested before being approved for clinical use, alternative treatments are not. Therefore, while the latter is labelled as “natural”, it may not necessarily be beneficial to the patient, and in some instances, may interfere with conventional treatment if taken concurrently. In addition to these products being consumed, South Africa is home to a large population of traders and collectors of medicinal plants who derive a livelihood from trading in these goods. There is therefore a great need not only to assess the clinical benefits of these products so that they can be administered safely and effectively, but also to provide support to TMPs to develop their practice in a sustainable and economically productive way.

### *1.5 Natural products as adjuvants for chemotherapy*

For many years natural products derived from medicinal plants have been researched and used in drug discovery. A few examples of common chemotherapeutic drugs derived from natural compounds include: 1) Paclitaxel - a terpenoid compound isolated from the bark and needles of the Pacific yew tree, *Taxus brevifolia*, and is used to treat breast cancer, ovarian cancer, lung cancer, and Kaposi Sarcoma (Success Story: Taxol, n.d.; Yang-Hua et al., 2020; Zhu and Chen, 2019); 2) Etoposide - a non-alkaloid lignan derivative isolated from the rhizomes and roots of the Mayapple, *Podophyllum peltatum*, or the *Podophyllum emodi* and is used in the treatment of a range of cancers including lung cancer, breast cancer, testicular cancer and non-Hodgkin lymphoma (Kluska and Woźniak, 2021; Thirumaran et al., 2007; Zhang et al., 2018); and 3) Vincristine - a vinca alkaloid isolated from the leaves of the Madagascar periwinkle, *Catharanthus roseus*, and is used for the treatment of non-Hodgkin lymphoma, breast cancer and leukemia (Dhyani et al., 2022; Škubník et al., 2021).

The intensive, high-dose treatment regimens used for the treatment of certain cancers such as Burkitt Lymphoma; breast cancer, etc., lead to patients suffering from severe side effects including nephrotoxicity, hepatotoxicity, and immunosuppression, which severely impacts quality of life (Lin et al., 2020; Majolo et al., 2019; Sharifi-Rad et al., 2019). Furthermore, one of the main obstacles to cancer therapy is chemoresistance and more specifically the development of multi-drug resistance (MDR) in cancer cells. This is a phenomenon whereby cancer cells develop resistance and stop responding to a variety of chemotherapeutic drugs, resulting in disease relapse, metastasis, and requiring even more intensive chemotherapy regimens (Hamed et al., 2019; Zheng, 2017).

Recent trials have assessed the effectiveness of combining natural products in a synergistic manner with current chemotherapeutic regimens to develop approaches that will improve patient outcome and lessen side effects. This combinatorial approach may allow for the targeting of multiple signaling pathways and lower drug doses which could mitigate side effects, the emergence of resistance, and increase therapeutic efficacy. In some instances, natural compounds have been shown to act as

chemosensitizers to reverse MDR by predisposing cancer cells to chemotherapeutic drugs and potentiating the anti-cancer effects of these drugs (Hamed et al., 2019; Hashem et al., 2022; Lin et al., 2019). This synergistic effect has been observed for curcumin, the active ingredient of the rhizome of the plant *Curcuma longa* (turmeric) and is commonly used as a food additive. Curcumin has been used for years in traditional Southeast Asian medicine and Indian folk medicine to treat a range of diseases, and found to have anti-cancer properties, such as inducing apoptosis and cell cycle arrest; and inhibiting cellular proliferation and invasion, in many different types of cancers. Recently, the antitumor efficacy of curcumin has been studied in combination with chemotherapeutic drugs such as cisplatin, doxorubicin, and etoposide (Baharuddin et al., 2015; Hosseinzadeh et al., 2011; Lin et al., 2019; Saleh et al., 2021; Zhao et al., 2018). A study conducted by Baharuddin et al. (2015) reported that curcumin may be useful as a complement to chemotherapy since it was shown to increase the efficacy of cisplatin against non-small cell lung cancer (NSCLC) cells in *in vitro* assays (Baharuddin et al., 2015). In a separate study by Zhao et al. (2018), curcumin was shown to induce DNA damage and caspase-3-dependent apoptosis in lymphoma cells, and to further sensitize these cells to the DNA-damaging drugs cisplatin and camptothecin (Zhao et al., 2018).

### *1.6 Dodonaea viscosa var. angustifolia*

South Africa has a rich diversity of cultures and indigenous plants - the Western Cape alone is said to have over 500 medicinal plants used by local traditional healers. Within the Western Cape, the medicinal plant industry is largely run and controlled, informally, by the Rastafari Bush doctors (Philander et al., 2014). The latter are neo-traditional healers as their practices stem from Xhosa, Zulu, and Khoi-San cultures. Unlike western medicine, traditional healers pass their vast knowledge of medicinal plants from elders and treat patients based on their symptoms only. The Rastafari Bush doctors harvest their medicinal plants from the wild and play a key role in preserving the South African indigenous knowledge and healing cultures (Philander et al., 2014; Petersen et al., 2014). Studies report that the integration of the traditional healer's knowledge of medicinal plants with western contemporary medicine is likely to be advantageous and improve knowledge and use of these natural products (Philander et al., 2014; Petersen et al., 2014).

*Dodonaea viscosa* var. angustifolia is an evergreen shrub found in various parts of the world but most notably in the tropical and subtropical regions of the Western Cape and has been used for many years by the Rastafari Bush doctors or "bossidokter" (in the local Afrikaans language) (Fig. 1.2). They gather medicinal plants from the wild, trade these with each other, and sell them to the public in both city environments and rural settings. The *D. viscosa* plant is most commonly administered as a tea (using the leaves and bark) to treat a range of ailments, including colds, influenza, stomach troubles, thrush,

and even measles (Anandan et al., 2019 and Ngabaza et al., 2017). The leaves are also indicated for use externally, as remedy for skin rashes and itchiness.

A B

**Figure 1.2: Images of the *Dodonaea viscosa var. angustifolia* plant (A), Rastafari Bush doctor / traditional healer selling their product (B).** Image A is adapted from Rautenbach et al. (Unpublished). Image B is adapted from www.health24.com/Natural/Natural-approach/African-traditional-medicine-better-than-pills-20140821.

To date, the therapeutic properties of the plant and its derivatives, as well as the mechanisms of action, remain largely undefined scientifically, despite recent studies on both the crude extract and bioactive compounds from the extract (Al-Snafi, 2017; Anandan et al., 2019; Hossain, 2018). These include reports on the anti-microbial potential of the crude extract, where the latter was demonstrated to have inhibitory effects on the growth and biofilm formation of a number of bacterial and fungal pathogens including *Streptococcus mutans*, *Candida albicans*, *Salmonella typhi*, *Shigella flexneri*, *Escherichia coli*, *Vibrio cholera*, *Mycobacterium tuberculosis* and *Pseudomonas fluorescens* (Al-Snafi, 2017; Anandan et al., 2019 Hamed Al Bimani, B. M. and Hossain, M. A, 2020; Jayaraman et al., 2021; Naidoo et al., 2012; Patel et al., 2013). *D. viscosa* methanolic extract was also demonstrated to have anti-diarrheal activity *in vivo*, where Swiss albino mice fed with various doses of the extract had delayed onset of castor oil-induced diarrhea (Abdela J, 2019). In a much earlier study, methanolic and chloroform extracts of *D. viscosa* was reported to have anti-HIV properties, where cells exposed to the virus displayed impaired syncytia formation (Rashed et al., 2013).

Several studies have reported on the antiproliferative effect of extracts of *D. viscosa* within the context of cancer (colon, lung, ovarian, cervical and breast). These have largely focused on assessing cell viability using MTT or similar assays, *in vitro*, without much insight into the mechanisms of action (Al-Musawi and Al-Saadi, 2021; Cao et al., 2009; Herrera-Calderon et al., 2020; Jayaraman et al., 2021; Mossa and Al-Shawi, 2015; Ramkumar et al., 2021). For instance, Al-Musawi and Al-Saadi (2021)

biosynthesized silver nanoparticles which incorporated the plant's leave extracts and showed that these particles inhibited the viability of lung and ovarian cancer cells in a dose-dependent manner (Al-Musawi and Al-Saadi, 2021). In another study, using MTT and trypan blue exclusion assays, the authors showed inhibitory action of *D. viscosa* leaf extracts on the breast cancer cell line MCF-7 (Jayaraman et al., 2021). In an earlier study, Mossa and Al-Shawi (2015) used Annexin V assays, cell morphology analysis (using microscopy) and cell cycle profiling to demonstrate that ethanolic extracts of *D. viscosa* could induce apoptosis, and cell cycle arrest in MDA-MB231 breast cancer cells (Mossa and Al-Shawi,2015). An important caveat of all of these studies is that the selectivity of the extract on the non-cancerous counterpart cells was not investigated.

To date, and to the best of our knowledge, there have been no studies investigating the anti-cancer effect of *D. viscosa* extracts on any type of lymphoma.

### *1.7 Aims of the study.*

This research aimed to investigate the anti-cancer potential of aqueous extracts of *D. viscosa* (DVE) on Burkitt lymphoma, an aggressive B-cell derived cancer, that is over-represented among the HIV infected population. This was achieved through the following specific objectives:

**Objective 1: To use various *in vitro* assays to assess the cytotoxic potential of aqueous extracts of DVE on two Burkitt Lymphoma (BL) cell lines, relative to a non-cancerous lymphoblastoid cell line.**

**Objective 2: To uncover the molecular pathway(s) mediating the cytotoxic activity of DVE in BL cells.**

**Objective 3: To use a xenograft immunocompromised BL mouse model to assess the effect of DVE on tumour development.**

# Chapter 2: Materials and Methods

## *2.1. Cell lines and culture conditions*

This study used two human Burkitt lymphoma cell lines (Ramos and BL41) and one EBV-immortalised lymphoblastoid cell line (L1439A). The Ramos cell line was obtained from the American Type Culture Collection (ATCC, USA), and is a B lymphocyte cell line that was derived from a 3-year-old, White, male patient with Burkitt's Lymphoma (American), and is EBV-negative. The BL41 cell line was kindly donated by Professor Dave Sandeep (Duke University, USA), and was originally established from the tumour tissue of an 8-year old boy with Burkitt Lymphoma and is EBV-negative. The Lymphoblastoid cell line (LCL), L1439A, was created by Ms. Ingrid Baumgarten from the Department of Chemical Pathology, University of Cape Town, using an adapted protocol from Freshney (2010), by infection, with EBV, of lymphoblasts donated by a healthy donor.

The Ramos and BL41 cell lines were cultured in Roswell Park Memorial Institute (RPMI-1640) media (Sigma-Aldrich, USA) supplemented with 10% fetal bovine serum (FBS) (ThermoFisher Scientific, USA) and 1% penicillin/streptomycin (P/S) solution (Sigma-Aldrich, USA). The L1439A cells were cultured in Dulbecco's Modified Eagles Medium (DMEM) (Sigma-Aldrich, USA) supplemented with 20% FBS and 1% P/S. All cell lines were incubated at 37$^{o}$C in a humidified incubator supplemented with 5% $CO_2$ and regularly tested for mycoplasma contamination to ensure that only mycoplasma-free cells were used in experiments. Mycoplasma testing involved culturing the cells in antibiotic-free medium for 2-3 days, thereafter the cells were fixed and stained with Hoechst 33342 stain solution (14533, Sigma-Aldrich, USA). Cells were then viewed and analyzed for the presence of mycoplasma using an inverted fluorescent microscope.

## *2.2 Freezing and Storage of cell lines*

For long-term storage, cells were resuspended in cold freezing media which consists of 10% cryo-preservative agent (either dimethyl sulfoxide (DMSO) or glycerol) and 10-20% FBS in RPMI or DMEM medium. Thereafter, the cells were aliquoted into cryovials (1ml) and transferred into a cell-freezing container (Nalgene® *Mr. Frosty*) which was thereafter stored at -80$^{o}$C overnight before being transferred under liquid nitrogen for long term storage.

## *2.3 Preparation of the Dodonaea viscosa aqueous extract*

The *Dodonaea viscosa* plant material was previously collected from the Stellenbosch area of the Western Cape region of South Africa during field trips (led by our collaborator Associate Professor Nokwanda Makunga based at Stellenbosch University). The plant material (bark and leaves) was air-dried and kept at room temperature (RT), similar to how the traditional healers store the plant.

The *Dodonaea viscosa* aqueous extract (DVE) was prepared by flash-freezing using liquid nitrogen and grinding into a fine powder. Five grams of the plant powder was transferred to an Erlenmeyer flask, and 50 ml of distilled water was added. The mixture was thereafter sonicated for 30 minutes and filtered twice using Whatman No. 1 filter paper, and the resulting extract was placed in a sonicator bath for 45 minutes. Aliquots of the extract were frozen at -80$^{o}$C, and thereafter freeze-dried to produce the DVE powder used in this study. The DVE powder was stored in an airtight light-safe metal container, containing silica beads, at room temperature.

### *2.4 Cell treatments with DVE*

Appropriate amounts of DVE powder were weighed and resuspended in sterile 1 x phosphate buffered saline (1x PBS). For all experiments (unless otherwise stated) cells were plated at a density of 1.6 x$10^5$ cells/ml at least 16 hours prior to the start of treatment. DVE treatment involved the addition of appropriate volumes of DVE stock solution directly to the medium to achieve the desired final concentration. Corresponding volumes of 1xPBS were added to cell dishes for use as controls.

### *2.5 WST-1 cell viability assay*

The WST-1 cell proliferation reagent (Roche Applied Science, Germany) was used to measure cell viability and determine the half-maximal inhibitory concentration of DVE in each of the cell lines. The WST-1 reagent is a tetrazolium salt that gets cleaved by mitochondrial dehydrogenases to formazan. Therefore, by measuring the amount of formazan formed, the number of metabolically active cells can be determined (Aykul and Martinez-Hackert., 2016). 1.6x$10^5$ cells/ml were plated in 96-well plates at least 16 hours before the start of treatment and treated with various concentrations of DVE (0, 0.08; 0.12; 0.16; 0.18; 0.22, 0.24, 0.26 and 0.3 mg/ml), and corresponding controls were included (1x PBS). After 24 hours of treatment, 10µL of WST-1 reagent was added to each well and the cells were incubated at 37$^{o}$C in a humidified incubator supplemented with 5% $CO_2$, for 2 hours. Thereafter, absorbance at 450nm was measured using a spectrophotometer (Glo-Max®-Multi+ multiplate reader, Promega, USA). For each experiment, triplicate wells were included, and at least three independent experiments were performed.

### *2.6 Determination of Selectivity index (SI)*

The SI was determined using the following equation:

$$SI = \frac{IC_{50}\ of\ the\ control\ cell\ line}{IC_{50}\ of\ the\ cancer\ cell\ line}$$

An SI value of >1 is favourable, as this indicates that the drug is selectively cytotoxic towards cancer cells. The higher the SI value of a drug is, the more selective it is towards cancer cells.

### *2.7 Colony forming assay in MethoCult*

The colony forming assay was performed using the methylcellulose-based semi-solid medium, MethoCult™ (STEMCELL Technologies, Canada). This medium contains cytokines and supplements to support the growth of Haematopoeitic-derived cells. Ramos and BL41 cells were counted and seeded at a density of $4x10^5$ cells /mL in MethoCult with or without DVE (Ramos – 0.06 mg/ml; and BL41 – 0.18 mg/ml), in a 35mm culture dish. Dishes were incubated at 37°C in a humidified incubator supplemented with 5% $CO_2$ for 7 days. On days 0, 4, and 7 the cells were visualized by light microscopy (Zeiss Axiovert 200M, Carl Zeiss Microimaging, Germany) and images captured at 10x and 20x magnification using the Zeiss AxioCam HRm camera.

### *2.8 Cell Trace CFSE assay*

The Cell Trace™ CFSE proliferation kit (ThermoFisher Scientific, USA) was used to label cells and trace multiple cell generations by flow cytometry. This kit contains one vial of lyophilized CFSE dye powder and a vial of DMSO. To prepare the CFSE dye stock solution, 18µL of DMSO was added to the lyophilized powder to make a 5mM stock solution.

Ramos and BL41 cells were counted using the Haemocytometer and $1x10^6$ cells per sample were transferred to a 15mL Falcon tube to be prepared for staining. The cells were then washed twice in cold 1x PBS and resuspended in 2mL 1x PBS. Thereafter the appropriate volume of dye was added to the cell suspension, to get a final working concentration of 0.5-1µM and allowed to incubate for 20 minutes at room temperature (protected from light) with gentle agitation. Five times the original staining volume of complete culture medium was added to the cells and incubated for 5 minutes at room temperature, to remove any free dye remaining in the solution. The cells were then centrifuged and resuspended in 4 mL pre-warmed complete culture medium and plated in duplicate in 6-well plates. Once plated, the appropriate wells were treated with 0.04 mg/ml DVE or treated with 1 x PBS (vehicle control) and incubated at 37°C in a humidified incubator supplemented with 5% $CO_2$, for 48 hours, in the dark. Parent cell generations were stained as described above and fixed immediately. For fixation, samples were transferred to 15mL Falcon tubes, pelleted, and resuspended in 1mL 1x PBS. Thereafter 3mL 70% Methanol was added dropwise, while gently vortexing to avoid clumping, and thereafter transferred to 5mL Falcon round bottom test tubes. These were incubated on ice for 30 minutes, washed twice in 1 x PBS, and resuspended in 200µL 1x PBS. For data capture, each cell line of 4 samples: vehicle-treated sample (48 hours), DVE-treated sample (48 hours), t=0 sample (parent cell generation), and lastly an unstained parent sample. Data was captured using the Becton Dickson FACSymphony™ A5 flow cytometry instrument (Becton Dickson, USA) and analysed using FlowJo v10.9.

### *2.9 Morphological assessment using light microscopy*

Ramos, BL41, and L1439A cells were counted using the Haemocytometer and plated in a 6-well plate at a concentration of 1.6 x$10^5$ cells/ml at least 16 hours prior to treatment. Cells were treated with DVE, at the calculated $IC_{50}$ value (L1439A – 0.1 mg/ml; Ramos – 0.06 mg/ml; and BL41 – 0.18 mg/ml), and vehicle (PBS) for 24 hours and incubated at 37°C in a humidified incubator supplemented with 5% $CO_2$. Thereafter, the morphology of the cells was observed using light microscopy (Zeiss Axiovert 200M, Carl Zeiss Microimaging, Germany) at 10x and 40x magnification. Pictures were captured using the Zeiss AxioCam HRm camera.

### *2.10 Annexin V detection assay*

The PE Annexin V apoptosis detection kit I (BD Biosciences, USA) was used to evaluate DVE's effect on apoptosis. This kit contains the Annexin V protein which is conjugated to the fluorochrome Phycoerythrin (PE), which binds to phosphatidylserine residues on the surface of apoptotic cells, and 7-Amino-Actinomycin (7-AAD), which binds to DNA strands by intercalating between base pairs in the G-C rich regions. Double staining with Annexin V and 7AAD is used to differentiate between early and late apoptotic cells, as cells with intact plasma membranes will stain positive for Annexin V only (early apoptosis), and cells that are Annexin V positive/7AAD positive are undergoing late apoptosis/necrosis as the plasma membrane are no longer intact and 7AAD is able to intercalate with exposed DNA strands (Annexin A5 affinity assay, 2017). The PE Annexin V apoptosis detection kit was used according to the manufacturer's instructions.

Ramos, BL41, and L1439A cells were counted using the Haemocytometer and plated in a 6-well plate at a concentration of 1.6 x$10^5$ cells/ml at least 16 hours prior to treatment with DVE (L1439A – 0.1 mg/ml; Ramos – 0.06 mg/ml; and BL41 – 0.18 mg/m) or vehicle (PBS). Following treatment for 24 hours, duplicate samples were pooled and washed twice with cold sterile 1x PBS. Thereafter the cells were pelleted and resuspended in 100µL of 1x Binding buffer to ensure a final total number of 1x$10^6$ cells per sample. Cell suspensions were thereafter transferred to 5 mL Falcon round bottom test tubes, and 5µL of PE Annexin V and 5µL of 7AAD were added to the appropriate tubes and incubated in the dark, at room temperature for 15 minutes. Each cell line contained 6 samples which consisted of: Untreated (stained with Annexin V and 7AAD); Treated (stained with Annexin V and 7AAD); 5% DMSO (stained with Annexin V and 7AAD); 5% DMSO (stained with Annexin V only); 5% DMSO (stained with 7AAD only); Negative control (Unstained healthy cells). Following incubation, 600µL of 1x Binding buffer was added to each tube and the data was captured on the Becton Dickson FACSCalibure™ Flow cytometry instrument (Becton Dickson, USA). All compensation and analysis were performed using the Becton Dickson Cell Quest Pro™ software (Becton Dickson, USA).

### *2.11 Caspase 3/7 assay*

The Caspase-Glo®3/7 kit was used to determine changes in caspase 3/7 activity in cells treated with DVE, relative to vehicle. This kit contains the Caspase-Glo®3/7 DEVD-aminoluciferin substrate and the Caspase-Glo® buffer, which was mixed together, according to the manufacturer's instructions, to form the Caspase-Glo®3/7 reagent. This assay measures caspase 3/7 activity through the cleavage of the DEVD aminoluciferin substrate by caspases 3 and 7, to release free aminoluciferin which is then consumed by luciferase to generate a luminescent signal that's proportional to the amount of caspase activity.

Cells were counted, using the Haemocytometer, and plated in a 96-well plate, at $1.6x10^5$ cells/ml at least 16 hours prior to treatment and incubated at 37°C in a humidified incubator supplemented with 5% $CO_2$. Cells were treated with their respective $IC_{50}$ values for DVE (L1439A – 0.1 mg/ml; Ramos – 0.06 mg/ml; and BL41 – 0.18 mg/m), for 24hrs. Thereafter 100uL of the Caspase-Glo®3/7 reagent was added to each well and the plate was incubated at 37°C in a humidified incubator supplemented with 5% $CO_2$, for 2 hours. Luminescent signal was then measured using the Glo-Max®-Multi+ multiplate reader (Promega, USA).

### *2.12 Western Blot analysis*

#### *2.12.1 Protein extraction and quantification*

Ramos, BL41, and L1439A cells were counted using the Haemocytometer and plated in a 6-well plate at a concentration of $1.6 x10^5$ cells/ml at least 16 hours prior to treatment. Thereafter, cells were treated with DVE, at the calculated $IC_{50}$ value (L1439A – 0.1 mg/ml; Ramos – 0.06 mg/ml; and BL41 – 0.18 mg/ml), and vehicle (PBS) for 24 hours and incubated at 37°C in a humidified incubator supplemented with 5% $CO_2$. Total protein was extracted using Radio-Immunoprecipitation Assay (RIPA) buffer including 1x complete™, mini EDTA-free Protease inhibitor (Roche, Germany). Thereafter the lysates were stored overnight at -80°C for optimum cell lysis, followed by centrifugation for 20 minutes at 12 000 rpm (at 4°C) to remove cell debris. The resulting supernatant (containing soluble protein) was aliquoted into 1.5 ml microcentrifuge tubes and stored at -80°C.

The Pierce™ bicinchonic acid (BCA) assay kit (ThermoFisher Scientific, USA) was used for protein quantification. This assay utilizes a colorimetric detection system based on the reduction of $Cu^{2+}$ to $Cu^{1+}$ by protein peptide bonds in an alkaline medium. The BCA molecules chelate with the reduced $Cu^{1+}$ to form a BCA/$Cu^{1+}$ complex that produces a purple colour, which is proportional to protein concentration. A standard curve was generated using the bovine serum albumin (BSA) absorbance readings at a range of concentrations, and the resulting linear plot was used to determine the protein concentration of each sample.

Protein samples and BSA standards were diluted (1:4), and 10µl aliquots were quantified in duplicate - 200µL of the prepared working reagent was added to sample in a 96-well plate; the latter was incubated for 30 minutes at 37°C and thereafter absorbance was measured at 560nm using the Glo-Max®-Multi+ multiplate reader (Promega, USA). The protein sample concentrations were then extrapolated from the BSA standard curve.

### *2.12.2 Protein separation using SDS-PAGE*

Protein samples were separated by molecular weight using sodium dodecyl sulphate-polyacrylamide gel electrophoresis (SDS-PAGE). The Mini-PROTEAN 3 system (Bio-Rad, USA) was used to prepare the electrophoresis gel which comprised of a 5% stacking gel and a 10-15% resolving gel.

All protein samples were prepared for loading by combining the following components, as shown in Table 2.1, Dithiothreitol (DTT), 5 x SDS loading dye and RIPA buffer. Thereafter, the samples were heated to 95°C for 5-10 minutes to denature the protein prior to loading. A PageRuler™ Prestained Protein Ladder (ThermoFisher™ Scientific, USA) was included in one of the lanes to accurately determine protein size. All samples were separated by electrophoresis in 1x Running buffer at 100V for 2.5 – 3 hours.

**Table 2.1: Protein sample preparation for SDS-PAGE**

| Component | Volume (µL) |
|---|---|
| **Protein (10 – 40 µg)** | X |
| **100 mM DTT** | 1 |
| **5 x SDS loading dye** | 6 |
| **RIPA Buffer** | Up to 25µL |

µL – microlitre; µg – microgram

### *2.12.3 Protein transfer onto nitrocellulose membrane and western blotting*

Following electrophoresis, the separated proteins on the SDS-PAGE gel were transferred onto nitrocellulose membrane (Bio-Rad, USA) using the Mini Trans-Blot® cell assembly (Bio-Rad, USA), with cold 1x Transfer buffer by electrophoresis at 100V for 1.5 hours.

Once the transfer was complete, the nitrocellulose membrane was washed in cold 1x Tris-buffered saline + 0.1% Tween-20 (TBST) or 1x PBS + 0.1% Tween-20 (PBST) with gentle shaking for 2 x 5-minute followed by 2 x 10-minute washes at room temperature. Thereafter, the membrane was incubated in blocking buffer (5% fat-free milk / 5% BSA in TBST/PBST) for 1 hour, with gentle agitation, followed by incubation in primary antibody diluted in blocking buffer overnight at 4°C, with gentle agitation. Table 2.2 outlines the primary antibodies (Cell Signaling Technology, USA) used in this study and their respective buffers and dilutions.

**Table 2.2: Primary and Secondary antibody dilutions and incubation buffers used for western blotting.**

| Protein | Buffer | Primary Antibody Dilution | Secondary Antibody Dilution |
|---|---|---|---|
| **Cleaved caspase 3** | 5% fat-free milk in 1xTBS/0.1% Tween-20 | 1:1000 | 1:5000 (Goat anti-rabbit) |
| **Cleaved PARP** | 5% BSA in 1xTBS/0.1% Tween-20 | 1:1000 | 1:3000 (Goat anti-rabbit) |
| **Total AKT** | 5% BSA in 1xTBS/0.1% Tween-20 | 1:1000 | 1:3000 (Goat anti-rabbit) |
| **Phospho-AKT (Ser 473)** | 5% BSA in 1xTBS/0.1% Tween-20 | 1:1000 | 1:3000 (Goat anti-rabbit) |
| **Phospho-PDK1** | 5% BSA in 1xTBS/0.1% Tween-20 | 1:1000 | 1:3000 (Goat anti-rabbit) |
| **Phospho-PTEN** | 5% BSA in 1xTBS/0.1% Tween-20 | 1:1000 | 1:3000 (Goat anti-rabbit) |
| **Phospho-GSK3β** | 5% BSA in 1xTBS/0.1% Tween-20 | 1:1000 | 1:3000 (Goat anti-rabbit) |
| **p38** | 5% fat-free milk in 1xPBS/0.1% Tween-20 | 1:1000 | 1:5000 (Goat anti-rabbit) |

After overnight incubation, the membrane was washed as previously described followed by incubation with the appropriate HRP-conjugated secondary antibody (Cell Signalling Technology, USA) (Table 2.2) diluted in blocking buffer for 1 hour at room temperature with gentle agitation. The membrane was then washed, as before, and visualised by chemiluminescence using the Clarity™ Western ECL Substrate (Bio-Rad, USA), as per the manufacturer's instructions. The membranes were exposed to x-ray film, which was then developed and fixed to visualise the protein signal. Densitometric analysis of the protein signal intensity was performed using ImageJ v1.8 software (NIH, USA) and protein expression levels was represented as a ratio of protein of interest/p38 loading control, this was then normalised to the vehicle treated samples.

### *2.12.4 Membrane stripping for reprobing*

The bound antibodies were removed from the nitrocellulose membrane by incubating in pre-heated stripping buffer (100 mM β-mercaptoethanol, 2% SDS, 62.5 mM Tris HCl) at 50$^{o}$C for 30 minutes, with brief gentle agitation every 10-minutes. The membranes were then washed with cold 1x PBS/0.1% Tween-20 or 1x TBS/0.1% Tween-20, with gentle agitation for 2x 10 minutes. Thereafter the membranes were re-processed for western blotting to detect the internal loading control, p38 (Sigma-Aldrich, USA).

### *2.13 Development and use of Ramos xenograft nude mouse model.*

#### *2.13.1 Ethical Statement*

All animals were housed, monitored, and experimentally handled in strict accordance with international guidelines (du Sert et al., 2020) approved by the University of Cape Town, Faculty of Health Sciences Animal Research Ethics Committee (AEC study No. 019/038). Considerations for the welfare of the animals and humane euthanasia were highly respected and adhered to during the course of the study.

#### *2.13.2 In vivo assay*

The Ramos Burkitt lymphoma cells were used to develop the xenograft model. Ramos cells (1 x $10^7$) suspended in saline were subcutaneously injected into the hind flank of 24 (12 male and 12 female) NOD SCID nude mice (6-8 weeks old). Two weeks post subcutaneous injection the mice were randomly divided into four groups of 6 mice (3 male and 3 female mice). Treatment group one received DVE daily (freshly prepared, for each treatment day, from lyophilized powder), at a concentration of 0.065 mg/g, via oral gavage, while the control group received equivalent volumes of saline. The DVE dosage was calculated using the human dosage (5.24 mg/kg/day), the $K_m$ factor and the body surface area of the animal to convert the human dosage to an appropriate mouse dosage (Reagan-Shaw et al., 2007). Treatment group two was administered Doxorubicin Hydrochloride (Dox) (Sigma-Aldrich, USA) once a week, at a concentration of 0.008 mg/g, via intraperitoneal injection, while the control group received an equivalent volume of distilled water via intraperitoneal injection. Dox dosage was determined according to what is recommended in the literature, which states that half of the equivalent human dosage (50 mg/$m^2$) is typically used (Coiffier et al., 2010). Throughout the study, the welfare of the mice was monitored daily, mice were weighed thrice a week, and once visible, tumours were measured using a vernier caliper thrice a week. Tumour size was extrapolated using the following formula:

$$Tumour\ volume\ (mm^3) = \frac{(length\ x\ width\ x\ width)}{2}$$

At the end of the study, all the mice were humanely euthanized using Halothane.

### *2.14 Statistical analyses*

Statistical analyses were performed using student t-tests and one-way analysis of variance (ANOVA) tests, and significance was accepted at $p<0.05$. All statistical analyses were determined using the GraphPad Prism software v9 (USA). Where statistical analyses are absent, a representative of the result has been presented. This is because while the general trend of the data for each experiment was reproducible, the fold changes varied from experiment to experiment for various reasons including age of DVE, performance of kit and/or antibody, etc.

# Chapter 3: Results

## *3.1 Assessment of cytotoxicity of D. viscosa aqueous extract (DVE) on BL cells using in vitro assays.*

### *3.1.1 Impact on viability and proliferation.*

#### *3.1.1.1 DVE is cytotoxic to BL cells and displays a favourable selectivity index.*

The effect of DVE on cell viability in culture over a 24-hour period was assessed using the WST-1 assay (section 2.5). This is a tetrazolium-based assay that measures the cleavage of the tetrazolium salt, WST-1, by mitochondrial dehydrogenases to formazan. Therefore, an increase in the amount of formazan formed is correlated to an increase in mitochondrial enzyme activity in viable cells, as a proxy of cell viability and proliferation (Aykul and Martinez-Hackert., 2016; Şen et al., 2016). A range of DVE concentrations was used (0.08 – up to 0.3 mg/ml), on three cell lines - these included two BL cell lines, namely Ramos and BL41, and the non-cancerous lymphoblastoid cell line, L1439A. This process allows for the identification of an IC50 value, which is the concentration of extract sufficient to inhibit half of the viability. The IC50 values can then be used to determine the selectivity index (SI) of DVE, which is an indication of cytotoxic selectivity against BL cells versus non-cancerous B cells (A favourable SI should be > 1).

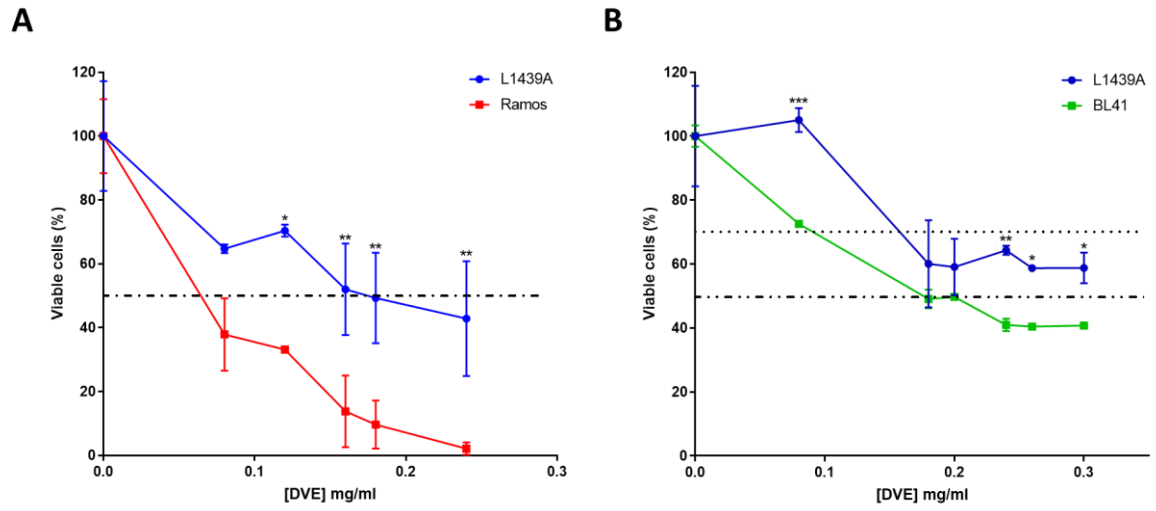


**Figure 3.1: IC50 and SI value determination of aqueous *D. viscosa* aqueous extract (DVE) using the WST-1 cell viability assay.** Burkitt lymphoma cells lines (A) Ramos and (B) BL41 and the control non-cancerous lymphoblastoid cell line, L1439A were treated with increasing concentrations of DVE (0.08 mg/ml – 0.3 mg/ml) and cell viability was measured after 24hrs of treatment, using the WST-1 assay. Data represents the mean ± Standard Deviation (N=3) for each concentration. Statistical analysis was determined by 2-way ANOVA using Šídák's multiple comparisons test on GraphPad Prism 9 software. P values are indicated as *p<0.05, **p<0.01, ***p<0.001. Experiments were performed at least in triplicate.

Shown in Figure 3.1 is a representation of the result obtained for this assay, which was performed at least in triplicate. Relative to the non-cancerous B cells (L1439A), both BL cell lines were significantly

more susceptible to loss of cell viability when exposed to DVE (Fig. 3.1). For instance, in the figure shown, the IC50 of Ramos cells is ~0.06 mg/ml, while that of L1439A is ~0.17 mg/ml (Fig. 3.1A). This translated to a very favourable selectivity index of 2.8 (IC50 value of L1439A / IC50 of Ramos),

While BL41 cells appeared to be less sensitive to DVE than Ramos cells, it was nevertheless more sensitive than the non-cancerous control cells. In that particular experiment, BL41 achieved an IC50 of 0.18 mg/ml (Fig. 3.1B), while L1439A did not achieve a loss in viability of greater than 50% throughout the range of DVE concentrations used. It must be mentioned that, although all experiments were performed using *D. viscosa* aqueous extract prepared from the same wild harvest, the potency appeared to vary, and the potential reasons for this variability will be discussed in Chapter 4. In the case of the BL41 cells, the IC30 value was used to determine the selectivity index of 1.7, which still indicates higher efficacy against this cell line relative to the non-cancerous B cells.

#### *3.1.1.2 DVE inhibits proliferation of BL cells in semi-solid medium.*

Having determined that DVE affects the viability of BL cells in a dose-dependent manner, and the IC50 established, the effect of DVE on cell proliferation was investigated. Traditional liquid cell culture media is designed to ensure continuous cancer cell proliferation and their composition does not recapitulate the tumours microenvironment. The use of a semi-solid matrix is known to be a closer mimic of the 3D cellular microenvironment that exists *in vivo*, and thus is widely used in cancer research to assess the ability of cancer cells to form colonies and propagate. While an agar-based medium is most popular for these assays, this was not suitable for the growth of lymphocyte cell lines, and thus a methylcellulose-based semi-solid medium (MethoCult) was used. MethoCult contains specific supplements and growth factors to support the growth of haematopoietic-derived cells (Human Colony-Forming Unit (CFU) Assays Using MethoCult™ Technical Manual, 2019) (section 2.7). Cells were seeded in MethoCult with and without the addition of DVE (Ramos - 0.06 mg/ml, and BL41 - 0.1 mg/ml) and allowed to grow over a period of 7 days. The ability of the cells to grow and form colonies in the semi-solid medium was monitored daily using light microscopy.

Shown in Figure 3.2 below are representative images of cell density at plating (Day 0), at Day 4 (approximately halfway through the experiment), and when the experiment was stopped (Day 7). The results clearly show that DVE has a negative impact on cell proliferation. In the absence of DVE, both Ramos and BL41 cells proliferated to form small colonies which increased in density over time (Fig. 3.2

– MethoCult without DVE images at Days 4 and 7), while in the presence of DVE, the cell density was severely diminished (Fig. 3.2 – MethoCult with DVE images at Days 4 and 7).

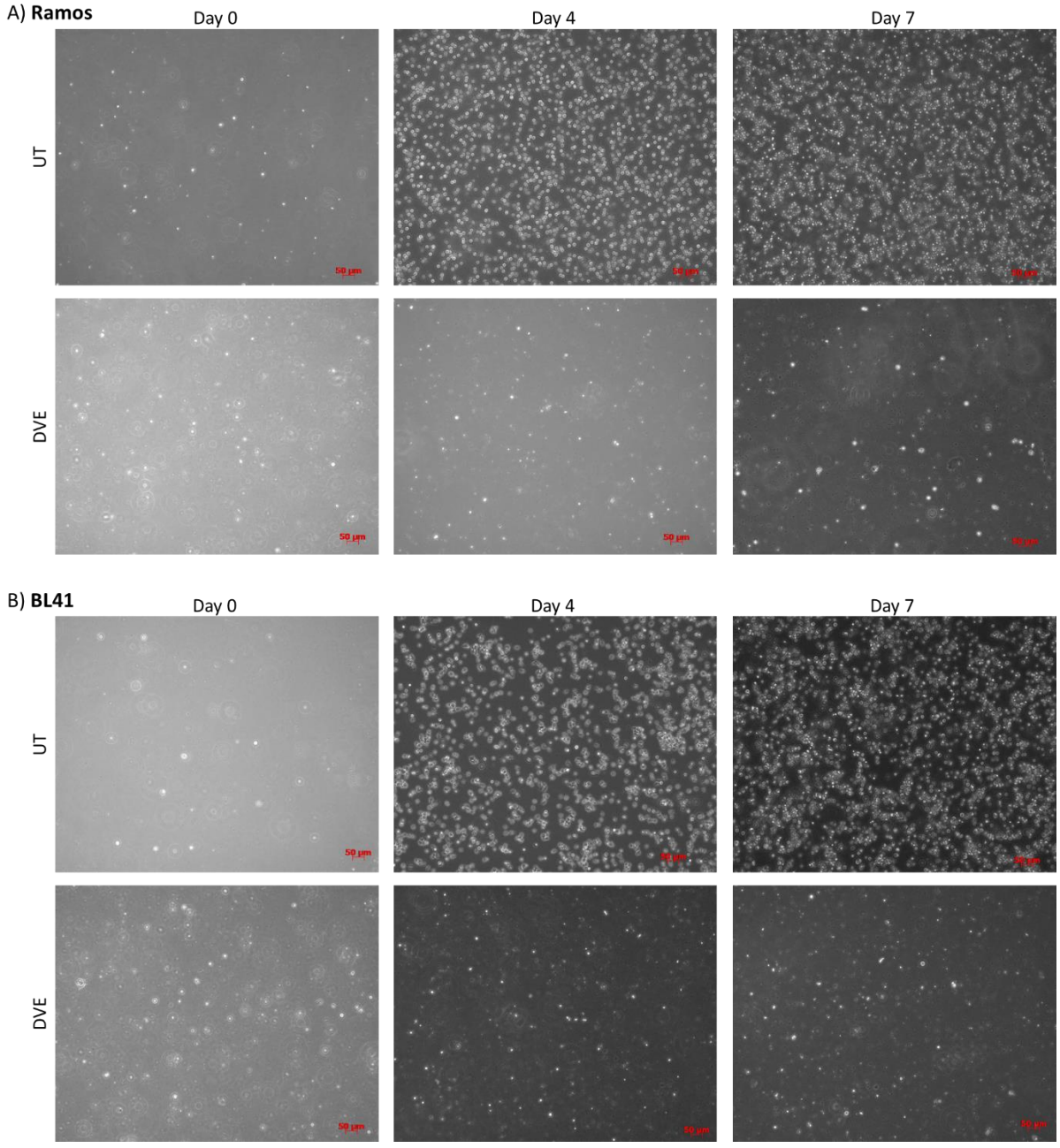


**Figure 3.2: Phase contrast images of Ramos and BL41 cells cultured in MethoCult semi-solid medium with or without DVE**. Burkitt lymphoma cell lines (A) Ramos and (B) BL41 were seeded in MethoCult with or without the addition of DVE (Ramos - 0.06 mg/ml and BL41 - 0.1 mg/ml) and allowed to grow for 7 days. Cell growth was assessed by light microscopy and images captured using a digital camera (Carl Zeiss Axiovert 200M) at x10 magnification on days 0, 4 and 7.

### *3.1.1.3 Proliferation-tracking experiment shows that DVE retards proliferation of BL cells.*

To confirm the negative impact of DVE on BL cell proliferation, a tracking experiment was performed whereby the rate of proliferation over a 48-hour period was measured. This was performed using the CFSE CellTrace assay (section 2.8) which utilizes a cell permeable dye, namely carboxyfluorescein succinimidyl ester (CFSE). At the start of the assay, CFSE is added to the cell culture medium where it diffuses into the cell cytoplasm and gets cleaved by intracellular esterases into a fluorescent compound that reacts with amine groups of proteins to form a stable amide bond thus allowing long term dye retention in the cell (Givan et al., 1999; Quah and Parish., 2012; Wallace et al., 2008). When a CFSE-labelled cell undergoes mitosis, the fluorescence intensity is halved in the daughter cell generation (P2) and all subsequent cell divisions will have half of the previous generations' dye. This can then be tracked using flow cytometry.

Ramos and BL41 cells were seeded, stained with CFSE, and then treated with 0.04 mg/ml DVE (controls received equivalent amounts of PBS). A concentration lower than IC50 was used for both cell lines since the aim was not to achieve cell death but rather to assess impact on proliferation, over a period of 48 hours. The results are shown in Figure 3.3 below - there was a ~3.2-fold reduction (~50%) in cells which has progressed to P2 in DVE-treated Ramos cells (Fig. 3.3A & C), compared to untreated cells. For the BL41 cells, the result was even more pronounced, whereby a ~10.9-fold reduction (~73%) in DVE-treated cells progressed to P2, relative to untreated cells, was observed (Fig. 3.3B & D). A third peak, which likely resulted from cellular debris (CD) as a result of apoptosis, was also recorded for both cell lines and are represented by a small third peak (labelled CD).

A)

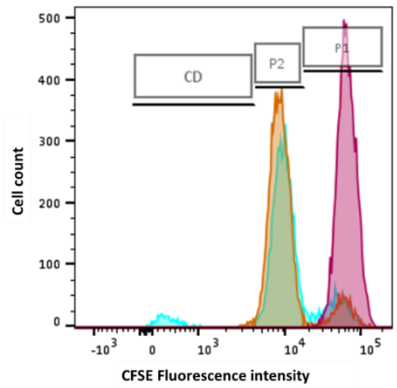


| | P1 (%) | P2 (%) | CD (%) |
|---|---|---|---|
| Ramos Day 0 | 99.7 | 0.088 | 0.22 |
| Ramos UT (48hr) | 11.4 | 87.5 | 1.10 |
| Ramos DVE (48hr) | 17.3 | 77.0 | 5.65 |

B)

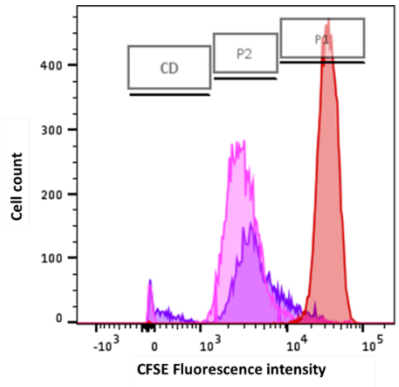


| | P1 (%) | P2 (%) | CD (%) |
|---|---|---|---|
| BL41 Day 0 | 99.6 | 0.13 | 0.29 |
| BL41 UT (48hr) | 5.78 | 88.7 | 6.33 |
| BL41 DVE (48hr) | 16.4 | 71.1 | 12.7 |

C)

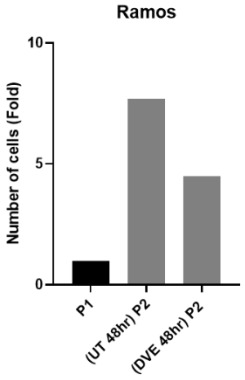


D)

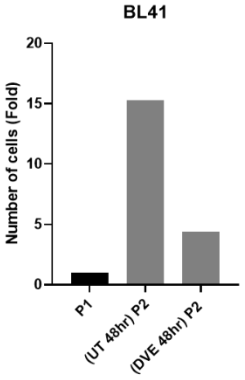


**Figure 3.3: Cell proliferation rate tracking using the CFSE Cell Trace assay.** Burkitt lymphoma cell lines Ramos (A) and BL41 (B) were stained with 1 µM CFSE Cell Trace dye, seeded and treated with vehicle (PBS) or DVE (0.04 mg/ml). After 48hrs, cells were fixed in 70% methanol, and samples were analysed by flow cytometry. A T=0 sample was included to track parent cell generation (P1) and daughter cell generation (P2). Data analyses were performed using the FlowJo v10.9 software. The assay was performed in duplicate.

### *3.1.2 Impact of DVE on apoptosis.*

#### *3.1.2.1 DVE-treated BL cells display typical apoptotic cellular morphology.*

Apoptosis, a programmed mode of cell death, is inhibited in cancer cells through diverse mechanism including the overexpression of anti-apoptotic proteins and the downregulation of pro-apoptotic proteins (Hanahan and Weinberg, 2011). In non-cancerous cells, this highly regulated process is triggered by a wide variety of conditions, including infectious agents, hypoxia, DNA damage, and more. Two main apoptotic pathways are described, namely the intrinsic and extrinsic pathways, with both converging towards the expression of executioner caspase proteins (caspase -3, -6 and -7), which are responsible for the cellular changes that occur during apoptosis (Pfeffer and Singh, 2018).

Cells undergoing apoptosis display typical morphological features which are described as the "morphological hallmarks of apoptosis" and include features such as cell shrinkage, chromatin condensation, nuclear fragmentation, and more (Banfalvi, 2017; Tixeira et al., 2017). These were assessed in cells treated with DVE (Ramos - 0.06 mg/ml, BL41 - 0.1 mg/ml and the non-cancerous control, L1439A - 0.1 mg/ml) for 24 hours and compared to untreated cells (section 2.9).

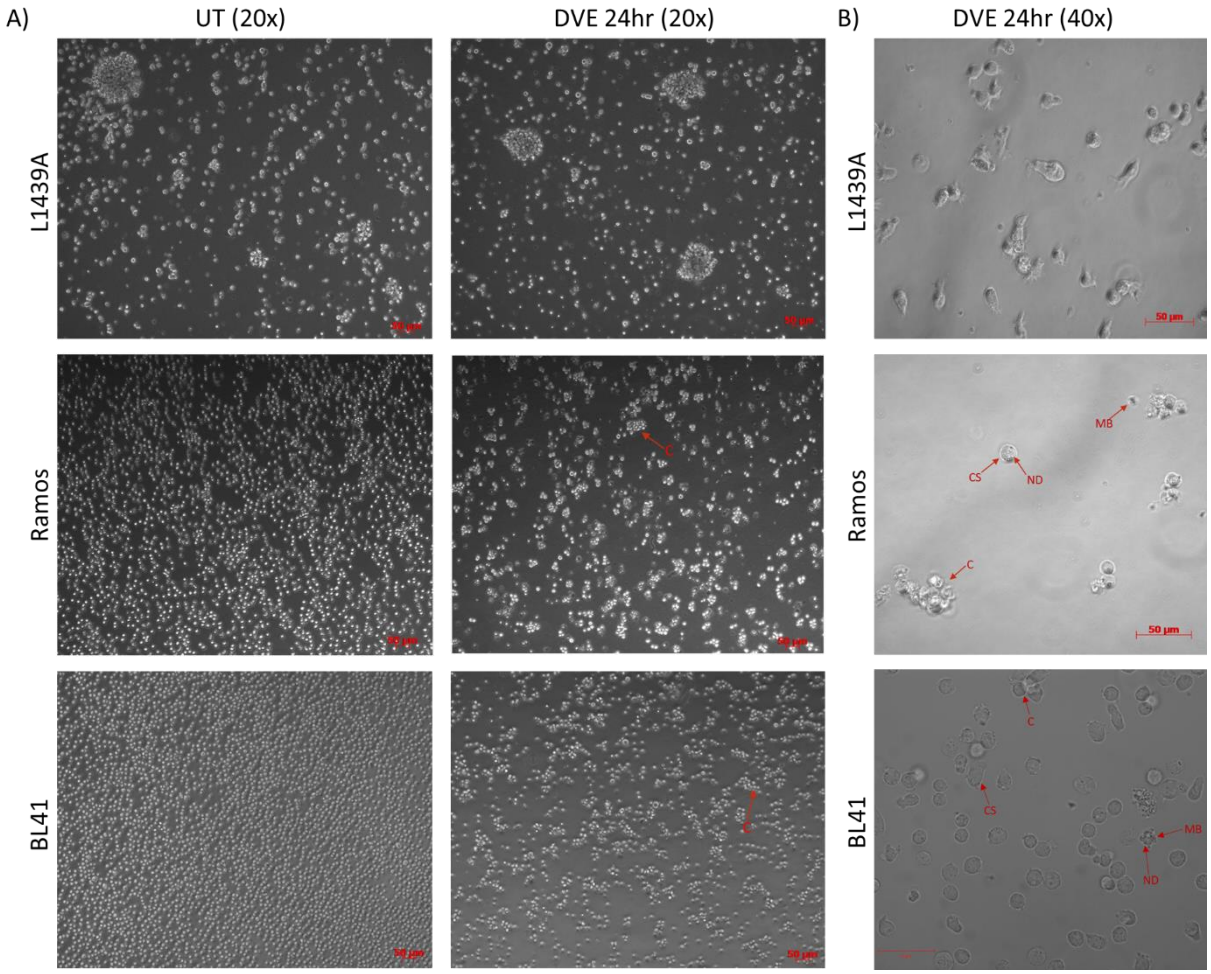


**Figure 3.4: Morphological changes associated with apoptosis in BL cells treated with DVE.** Burkitt Lymphoma cells (Ramos and BL41) and the non-cancerous lymphoblastoid control cells (L1439A) were treated by vehicle (PBS) or DVE (Ramos – 0.06 mg/ml; BL41 – 0.1 mg/ml) for 24hrs, and cell morphology was analysed using light microscopy. (A) Phase contrast images at x20 magnification. (B) Phase contrast images at x40 magnification. Clumping (c), cell swelling (CS), membrane blebbing (MB) and nuclear dissolution (ND). This experiment was performed at least in triplicate.

As shown in Figure 3.4A, the density of the non-malignant lymphoblastoid cells L1439A remained unchanged both in the presence and absence of DVE (Fig. 3.4A – top panels), and when observed at higher magnifications, no notable changes in cell morphology were observed between treated (DVE) and untreated (UT) cells, and a higher magnification of DVE-treated L1439A cells is shown in Figure 3.4B (upper panel). It is important to note that L1439A cells typically form large clumps, with smaller clumps and single cells (some round and some elongated) scattered throughout the medium.

In contrast, BL cells treated with DVE formed small clumps in the presence of DVE (Fig. 3.4 A – middle and lower panels). Under normal conditions, these cells typically growth as a single celled population with no clumps. Clumping is a typical feature of apoptosis of cells which usually grow as single cell suspension (Satoh et al., 2003). At higher magnifications (x40), while untreated cells looked round and

shiny, cells treated with DVE displayed cell swelling (CS), membrane blebbing (MB) and nuclear dissolution (ND) (Fig. 3.4B – middle and lower panels).

### *3.1.2.2. Annexin V assay show significant and selective DVE-induced cell death of BL cells.*

A cell's plasma membrane is a highly organized asymmetrical system. The membrane consists of two leaflets that are composed of different phospholipids, glycans and proteins on each side. The outer leaflet contains phosphatidylcholine (PC) and sphingomyelin (SM) whereas phosphatidylethanolamine (PE), phosphatidylserine (PS) and phosphatidic acid (PA) are mostly located on the inner leaflet. During apoptosis, this asymmetry is disrupted, and the plasma membrane undergoes structural changes to allow for the clearance of apoptotic cells by phagocytes. One of these changes includes the translocation of PS on the outer leaflet of the membrane, thereby exposing PS to the external cellular environment (Bailey et al., 2009; Demchenko, 2012). The Annexin V protein binds with high affinity to PS and this has been exploited to develop the Annexin V assay used to quantitatively assess apoptosis. In the current assay, the PE Annexin V detection kit (BD Biosciences, USA) was used - it contains a fluorochrome-conjugated Annexin V protein used to tag and detect early apoptotic cells, while late apoptotic/necrotic cells are detected using 7-Amino-Actinomycin (7-AAD), which is a fluorescent compound that binds to DNA strands by intercalating between base pairs in G-C rich regions (section 2.10). Thus, cells positive for Annexin V-positive and negative for 7AAD are classified as early apoptotic, while cells positive for both are classified as late (end-stage) apoptotic. Cells positive for 7AAD only are considered to be fully necrotic, or heavily damaged.

Cells were treated with DVE (Ramos - 0.06 mg/ml, BL41 - 0.1 mg/ml and the non-cancerous control, L1439A - 0.1 mg/ml) for 24 hours. As can be observed in Figure 3.5 below, DVE induces significantly more apoptosis and necrosis in the lymphoma cells with an ~8-fold increase in early apoptotic cells and a ~5-fold increase in late apoptotic cells for Ramos, and a ~20-fold increase in early apoptotic cells and a ~12-fold increase in late apoptotic cells for BL41, compared to a less pronounced effect observed in the lymphoblastoid control cells, i.e., ~2-fold increase in early and late apoptotic cells (Fig. 3.5B).

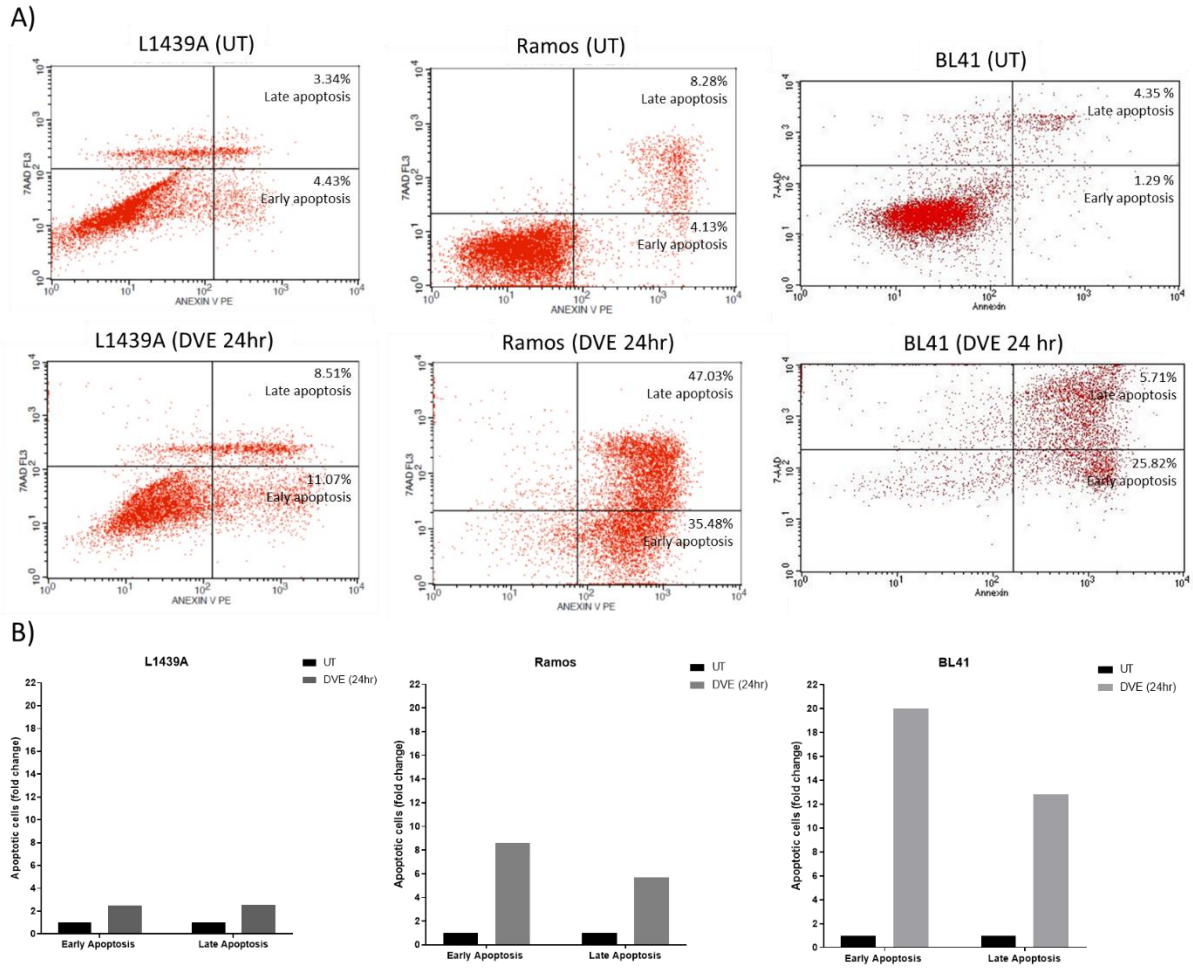


**Figure 3.5: Analysis of Annexin V/7AAD staining using flow cytometry to evaluate DVE-induced cell death in DVE-treated BL cells relative to untreated and compared to a non-cancerous cell line**. Burkitt lymphoma cells (Ramos and BL41) and the non-cancerous lymphoblastoid control cells (L1439A) were treated with vehicle (PBS) or DVE (L1439A – 0.1 mg/ml; Ramos – 0.06 mg/ml; BL41 – 0.1 mg/ml). After 24hrs, cells were harvested and stained with Annexin V and Propidium Iodide (PI) and data was captured by flow cytometry (A) and analysed using the GraphPad Prism 9 software (B). These experiments were performed in duplicate.

### *3.1.2.3. DVE significantly and selectively enhances Caspases 3 and 7 activity in BL cells.*

Caspases are a family of proteases which contain cysteine residues on their active sites and cleave protein substrates to activate or inactivate downstream signalling molecules. They play an important role in regulating and maintaining apoptotic, inflammatory, and developmental pathways. Apoptotic caspases are broadly classified as either initiator (caspase -2, -8, -9 and -10) or effector (caspase -3, -6 and -7) caspases, based on their mechanisms of action (McIlwain et al., 2013; Shalini et al., 2014). Initiator caspases have long N-terminal prodomains (100-200 amino acids), are structurally similar, and are activated through the intrinsic and extrinsic apoptotic pathways. Whereas effector caspases, common to both apoptotic pathways, have short N-terminal prodomains (±20 amino acids) and are cleaved by initiator caspases to their active forms. Once activated, they target specific cellular

substrates, ultimately resulting in cell death (Fiandalo and Kyprianou, 2012; Parrish et al., 2013; Savitskaya and Onishchenko, 2015).

The caspase-Glo® 3/7 assay (Promega, USA) (section 2.11) was used to measure changes in the activities of effector caspases 3 and 7 in cells exposed to DVE. The assay consists of a luminescent caspase 3/7 DEVD-amino luciferin substrate and a caspase-Glo buffer reagent that is optimised for cell lysis, caspase 3/7, and luciferase activity. Cleavage of the substrate by caspase 3/7 releases the DEVD-amino luciferin, which is then consumed by the luciferase to generate a luminescent signal that is proportional to caspase 3/7 activity.

Cells were treated with DVE (Ramos - 0.06 mg/ml, BL41 - 0.1 mg/ml and the non-cancerous control L1439A - 0.1 mg/ml) for 24 hours. As can be observed in Figure 3.6 below, no significant increase in caspase 3/7 activity was observed upon DVE treatment of the non-cancerous lymphoblastoid control cells (L1439A), while a significantly higher increase in activity of ~9-fold was observed for Ramos cells treated with 0.06 mg/ml DVE, compared to untreated cells (Fig. 3.6A). For BL41, the trend showed a general increase in caspase 3/7 activity, although this result was highly variable between replicates (Fig. 3.6B).

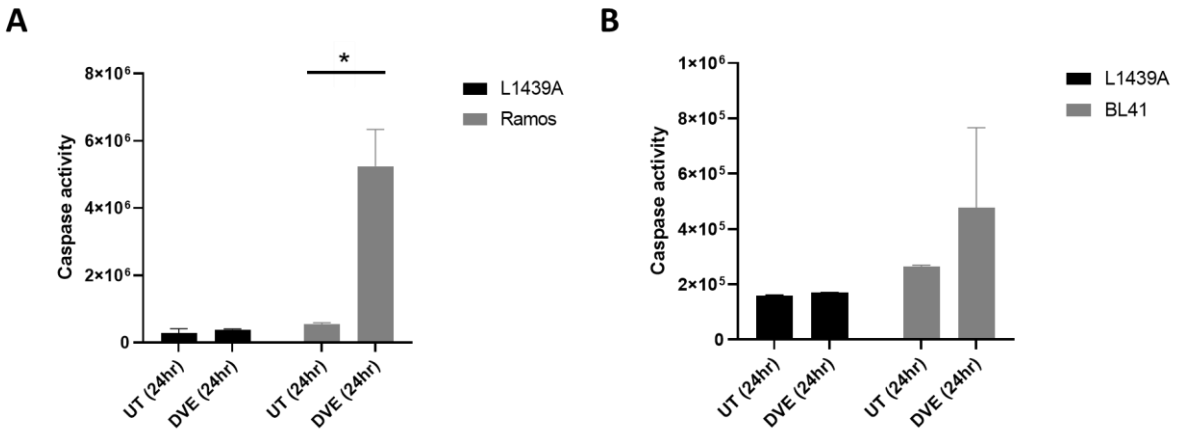


**Figure 3.6: Measure of Caspase 3/7 activity in BL and non-cancerous cells treated with DVE relative to untreated.** Burkitt Lymphoma cells (Ramos and BL41) and the non-cancerous lymphoblastoid control cells, L1439A (0.1 mg/ml), were treated with either vehicle (PBS) or DVE (Ramos – 0.06 mg/ml; BL41 – 0.1 mg/ml) for 24hrs. Thereafter, the caspase-Glo reagent was added, and luminescence was measured after 2hrs on a GloMax® Multi system. Data represents the mean ± standard deviation (N=2). Statistical analysis was determined by unpaired T-test using the Holm-Šídák method on GraphPad Prism 9 software. P values are indicated as *p ≤ 0.05. The experiments were performed at least in duplicate.

### *3.1.2.4. DVE significantly and selectively enhances cleaved caspases 3 and cleaved PARP1 protein levels in BL cells.*

Further experiments were performed to confirm the selective induction of apoptosis by DVE in BL cells, relative to a non-cancerous lymphoblastoid cell line. Using western blot analysis, the expression of two important effectors of apoptosis, namely cleaved caspase-3 (the active form of caspase-3; 17-19 kDa) and a major downstream target of caspase-7, namely cleaved poly (ADP-ribose) polymerase (PARP-1) (active form; 89 kDA), were measured in the three cell lines.

Cells were treated with DVE (Ramos - 0.06 mg/ml, BL41 - 0.1 mg/ml and the non-cancerous control L1439A - 0.1 mg/ml) for 24hrs, thereafter total protein was harvested, and western blot was performed (section 2.12). Upon DVE treatment, there was a significant increase in cleaved caspase-3 expression in both the Ramos and BL41 cells, relative to vehicle-treated cells (Fig. 3.7). No cleaved caspase-3 could be detected in the non-cancerous L1439A cells under both DVE-treated and vehicle-treated conditions, while the protein could be detected in vehicle-treated BL41 cells, although a notable increase is seen in DVE-treated cells (~1.4 fold).

When probed for the expression of cleaved PARP, none was detectable in all 3 cell lines treated with vehicle, as well as for DVE-treated L1439A, while a notable increase was seen for DVE-treated Ramos and BL41. The p38 map kinase protein (unphosphorylated) was used to demonstrate equal protein loading – this protein has been described as a reliable marker of protein loading for western blots (Hammond et al., 2020).

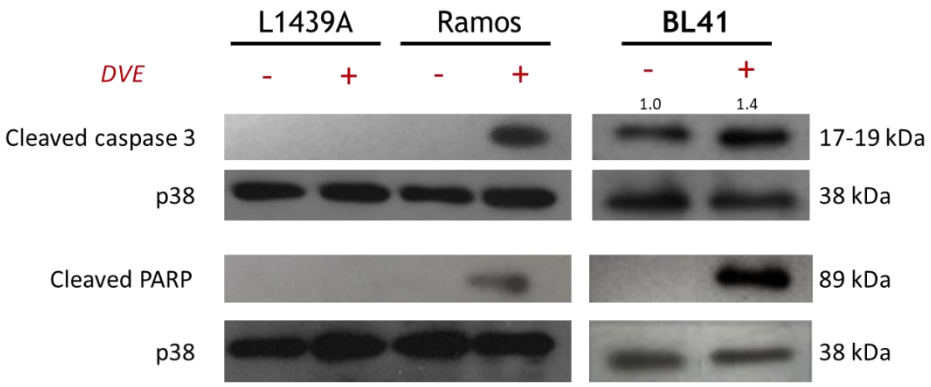


**Figure 3.7: Expression of cleaved caspase 3 and cleaved PARP upon DVE treatment in BL cells, and the lymphoblastoid cell line L1439A.** Burkitt Lymphoma cells (Ramos and BL41) and the non-cancerous lymphoblastoid control cells, L1439A, were treated with vehicle (PBS) or DVE (L1439A – 0.1 mg/ml; Ramos – 0.06 mg/ml; BL41 – 0.1 mg/ml) for 24hrs. Thereafter, total protein was extracted, and western blot was performed using anti-cleaved-caspase3 and anti-cleaved-PARP antibodies. The anti-p38 antibody was used as a loading control. Densitometric analysis was performed using ImageJ software and normalized to the loading control, p38. Fold increase was obtained by comparing the relative densitometric value of the DVE-treated BL41 cells to the vehicle-treated cells, which were set to 1. The experiments were performed at least in duplicate.

## 3.2 Cytotoxic mechanism of action of DVE in Burkitt Lymphoma cells.

Defining the mechanism of action of an anti-cancer drug is important for several reasons, one of which is that it provides important information about the safety of the drug, and how it may affect cellular processes, and the body (Aung et al., 2017). Furthermore, because cancer therapy involves the use of a combination of drugs, it is desirable that the mechanisms of cancer cell toxicity by the various drugs are different, to ensure that cells and molecules are targeted via more than one route.

The PI3K/AKT/mTOR pathway is frequently shown as essential in supporting the growth, survival, and proliferation of lymphoma cells (Bhatti et al., 2018; Sander et al., 2012; Schmitz et al., 2012). In fact, this pathway is a favourable therapy target for several cancers, including BL (Rohde et al., 2017; Schmitz et al., 2014). To assess whether the negative impact of DVE on cell viability is through the PI3K pathway, the expression of key components of the pathway was investigated upon DVE treatment.

Several major upstream activators of the PI3K/AKT/mTOR signalling pathway have been identified and include the receptor tyrosine kinases (RTKs), G-protein coupled receptors (GPCR), Toll-like receptors (TLRs) and B cell receptors (BCRs). Upon activation, PI3K acts as a lipid kinase to phosphorylate phosphoinositides leading to the conversion of phosphatidylinositol-4,5-bisphosphate (PIP2) to phosphatidylinositol-3,4,5-triphosphate (PIP3). A crucial mediator of PI3K is AKT (isoforms AKT1/2/3), which gets activated through phosphorylation (primarily at Thr*308* and Ser*473*) by PIP3 via 3-phosphoinositide-dependent kinase 1 (PDK1). This process can be inhibited by phosphatase and tensin homolog PTEN, which therefore acts as a tumour suppressor. Upon activation, AKT has the ability to phosphorylate multiple downstream targets, one of which is glycogen synthase kinase 3 (GSK3). The latter (both GSKα and GSKβ isoforms) becomes inactivated upon AKT induced phosphorylation and is targeted for proteasomal degradation. The mTORC2 (mammalian target of rapamycin complex 2) is considered an atypical member of the P13K related kinase family and has also been shown to phosphorylate AKT (Jellusova and Rickert, 2016; Morgensztern and McLeod, 2005).

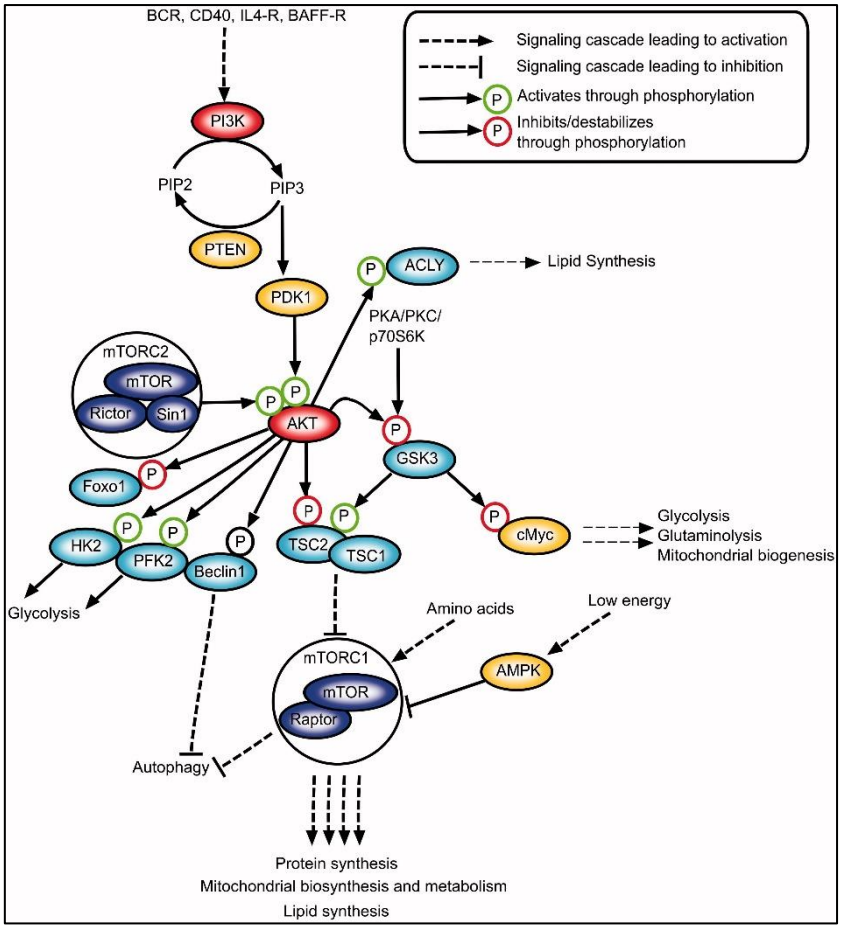


**Figure 3.8: Schematic representation of key proteins involved in the PI3K/AKT pathway**. Upstream regulators lead to PI3K-mediated phosphorylation of PIP2 to PIP3. The latter promotes AKT phosphorylation and activation via PDK1. AKT is also targeted for phosphorylation by the mammalian target of rapamycin complex 2 (mTORC2). Activated Akt is able to phosphorylate a range of targets involved in various metabolic processes including glycolysis, autophagy, cellular metabolism, lipid synthesis, and more. (Figure adapted from Jellusova and Rickert, 2016)

For this analysis, the expression of a number of key components of the pathway was assessed using western blotting. These included total AKT and phosphorylated AKT (Ser473), phosphorylated PTEN (Ser380), phosphorylated PDK1 (Ser241), and phosphorylated GSK3β (Ser9). BL cells were treated with DVE (Ramos – 0.03 and 0.06 mg/ml; and BL41 - 0.05 and 0.1 mg/ml) for 24hrs, thereafter total protein was harvested, and western blot was performed (section 2.12).

In both cell lines, treatment with DVE led to an increase in p-PTEN, the primary antagonist of the PI3K pathway (Fig. 3.9A and 3.10A). Specifically, a ~1.49-fold increase in p-PTEN was recorded in 0.06 mg/ml DVE-treated Ramos cells, and a ~1.65-fold increase was recorded in 0.05mg/ml DVE-treated BL41 cells, relative to untreated cells. The expression of p-PDK1, a direct target of PIP3, which is itself dephosphorylated by p-PTEN, was notably inhibited upon DVE treatment in Ramos cells (Fig. 3.9B), while the same was not observed in BL41 cells (Fig. 3.10B). Though the total amount of AKT increased

in DVE-treated Ramos cells (~1.45-fold increase at 0.03 mg/ml DVE and ~1.89-fold increase at 0.06 mg/ml DVE - Fig. 3.9C), phosphorylated AKT, which is a substrate of p-PDK1, was undetectable (data not shown). In contrast, in BL41 cells, the expression of both total AKT and phosphorylated AKT increased upon DVE treatment: total AKT increased by ~3.41-fold with 0.05 mg/ml DVE, and by ~1.73-fold with 0.1 mg/ml DVE while p-AKT(Ser473) increased by ~2.88-fold and ~7.56-fold with 0.05 mg/ml and 1 mg/ml DVE, respectively (Fig. 3.10C). Finally, upon assessment of changes in expression of p-GSK3β, a downstream target of phosphorylated AKT, the following was observed: in Ramos cells p-GSK3β expression was increased by ~1.75-fold with 0.06 mg/ml DVE, while a negligible decrease was seen with 0.03 mg/ml DVE (Fig. 3.9D) additionally, in BL41 cells, p-GSK3β protein levels were increased by ~2-fold and ~3-fold with 0.05 mg/ml and 0.1 mg/ml DVE, respectively (Fig. 3.10D).

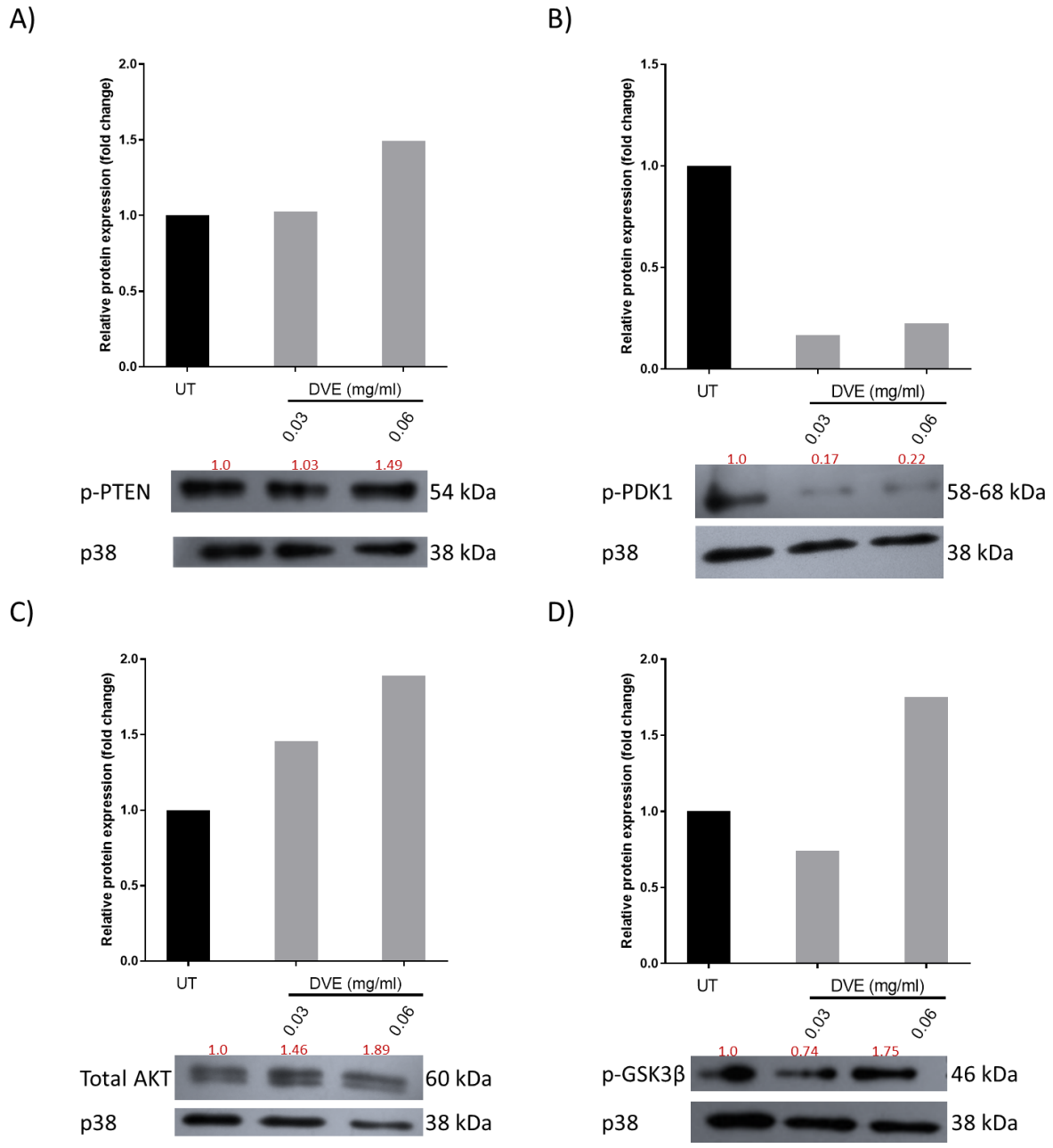


**Figure 3.9: Changes in expressions of key markers of the PI3K/Akt signaling pathway in DVE-treated Ramos cells.** Ramos cells were treated with vehicle (PBS) or DVE (0.03 mg/ml and 0.06 mg/ml) for 24hrs. Thereafter, total protein was harvested, and western blot was performed using anti p-PTEN (A), anti p-PDK1 (B), anti AKT (C) and anti p-GSK3β (D) antibodies. The total p38 protein was detected and used as a loading control. Bar graphs represent densitometric analysis. Densitometric analysis was performed using ImageJ software and normalized to the loading control. Fold increase was obtained by comparing the relative densitometric value of the DVE-treated Ramos cells to the vehicle-treated cells, which were set to 1, and the values indicated in the figure. The experiments were performed in duplicate.

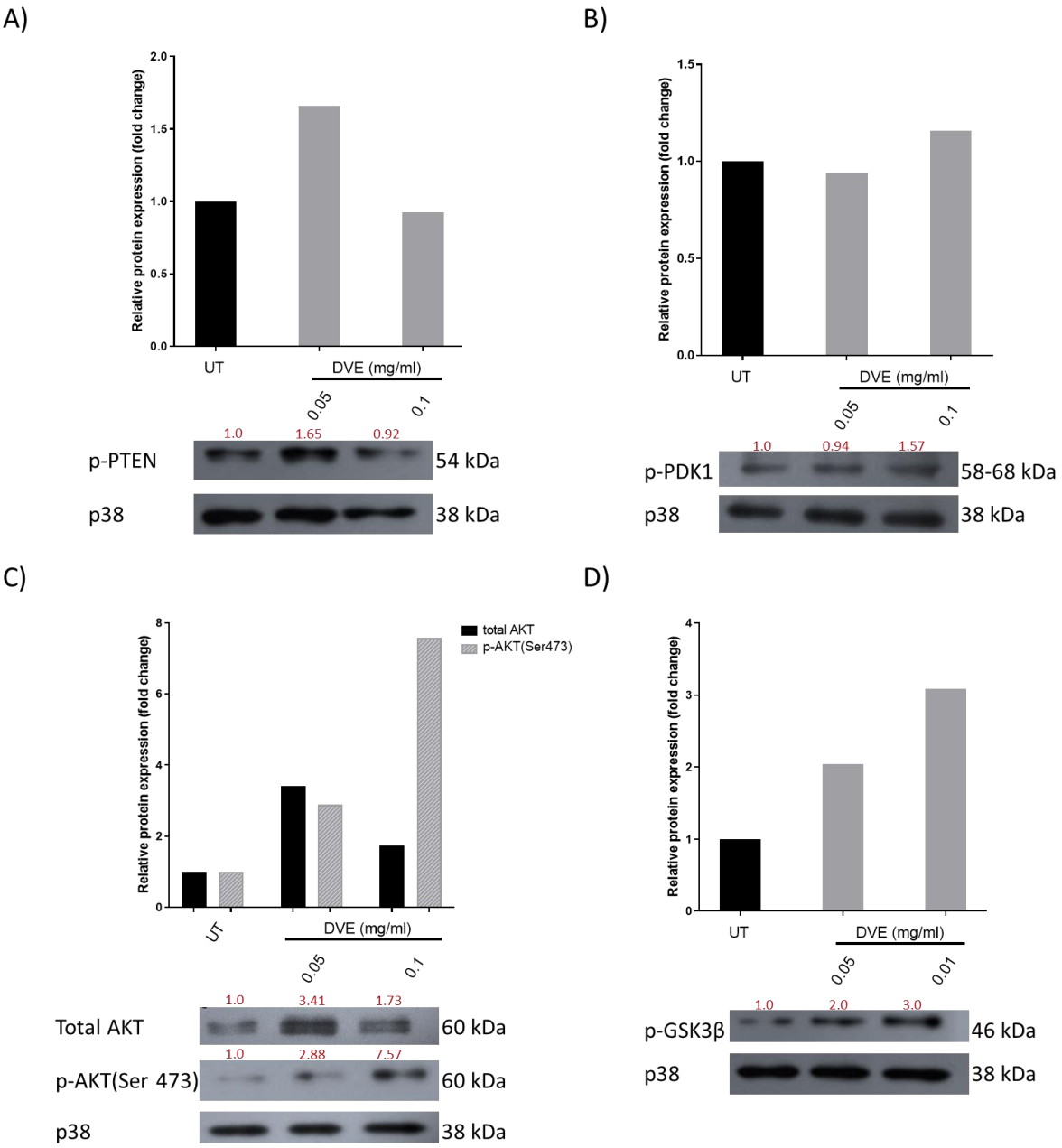


**Figure 3.10: Changes in expressions of key markers of the PI3K/Akt signaling pathway in DVE-treated BL41 cells.** BL41 cells were treated with vehicle (PBS) or DVE (0.05 mg/ml and 0.1 mg/ml) for 24hrs. Thereafter, total protein was harvested, and western blot was performed using anti p-PTEN (A), anti p-PDK1 (B), anti AKT (C), anti p-AKT(Ser 473) and anti p-GSK3β (D) antibodies. The total p38 protein was detected and used as a loading control. Bar graphs represent densitometric analysis. Densitometric analysis was performed using ImageJ software and normalized to the loading control. Fold increase was obtained by comparing the relative densitometric value of the DVE-treated BL41 cells to the vehicle-treated cells, which were set to 1, and the values indicated in the figure. The experiments were performed in duplicate.

### *3.3 The effect of DVE on tumour formation in a BL xenograft mouse model.*

Xenograft mouse models have been highly useful in cancer research (Jung, 2014). While the use of cells grown in culture as models to study the cytotoxicity of new drugs is a good starting point, it does not accurately represent the complexity of *in vivo* environments where many other influences come into play, the tumour microenvironment being one of the main factors. The immunocompromised nude mouse model has proven to be useful as a pre-clinical model, and is a widely used, to assess the safety and efficacy of potential anti-cancer drugs on human cancer cells / cell lines, through the development of xenografts.

#### *3.3.1 Establishment of a BL xenograft model - tumours develop faster in male, compared to female nude mice.*

While there are numerous published reports demonstrating that the BL cell line Ramos can successfully form tumours in the flanks of mice when injected subcutaneously, it was important that this was verified, and the correct conditions established within our own setting. Following animal ethics approval of this study (AEC ref no. 019_038 – pilot study), Ramos cells were subcutaneously injected into the hind flank of male (n=2) and female (n=2) nude mice, and tumour establishment was observed over a period of 2 weeks. At the end of the 2-week period, the mice were euthanised (section 2.13). Noticeable tumours were observed in 3 of the 4 mice, with relatively large tumours observed in both of the male mice, compared to the female mice (Fig. 3.11A and B). In the latter, a very small and barely distinguishable tumour formed in only one of the female mice (Fig. 3.11A – circled in red).

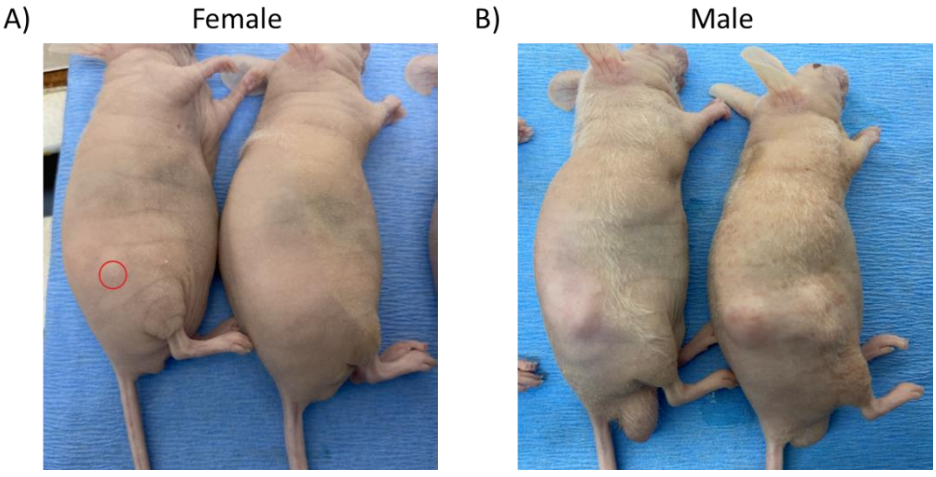


**Figure 3.11: Images of euthanized nude mice, two weeks post subcutaneous injection in the hind flank with Ramos cells.** 1 x $10^7$ Ramos cells were subcutaneously injected into the hind flank of female (n=2) and male (n=2) nude mice. Tumour formation was observed over a period of two weeks. Thereafter mice were humanely euthanized. One female (A) and two males (B) developed visible tumours over that time period.

### *3.3.2 Design of experimental study.*

Having successfully established a Ramos xenograft nude mouse model, the experimental plan, to use this model to assess the effect of DVE on tumour development, was developed. This is illustrated in Figure 3.12 below. A total of 24 mice were used (12 M and 12 F), and at 6-8 weeks of age, Ramos cells were (1 x $10^7$ cells) injected in the hind flank via subcutaneous injection. Two weeks later, the mice were randomized and grouped into four groups of six mice (3 males and 3 females) in each group. Test group 1 received DVE daily via oral gavage at 0.065 mg/g, and the control arm (Control group 1) received the equivalent volume of saline (Fig. 3.12). A positive control group was included whereby the mice received the chemotherapeutic drug Doxorubicin (Dox) (0.008mg/g) once a week via intraperitoneal injection (Test Group 2), and the corresponding control arm (Control group 2), received the equivalent volume of distilled water. Dox forms part of the standard chemotherapeutic regimen administered to Burkitt lymphoma patients (Atallah-Yunes et al., 2020). In addition to serving as a positive control, the inclusion of Dox is expected to provide insight on the safety profile of DVE, relative to Dox (which is linked to adverse events in both animal models and in human) (Matesun et al., 2022). The DVE dosage was calculated using the human dosage (5.24 mg/kg/day), the $K_m$ factor and the body surface area of the animal to convert the human dosage to an appropriate mouse dosage (Reagan-Shaw et al., 2007). Whereas the Dox dosage was determined according to what is recommended in the literature, which states that half of the equivalent human dosage (50 mg/$m^2$) is typically used (Coiffier et al., 2010).

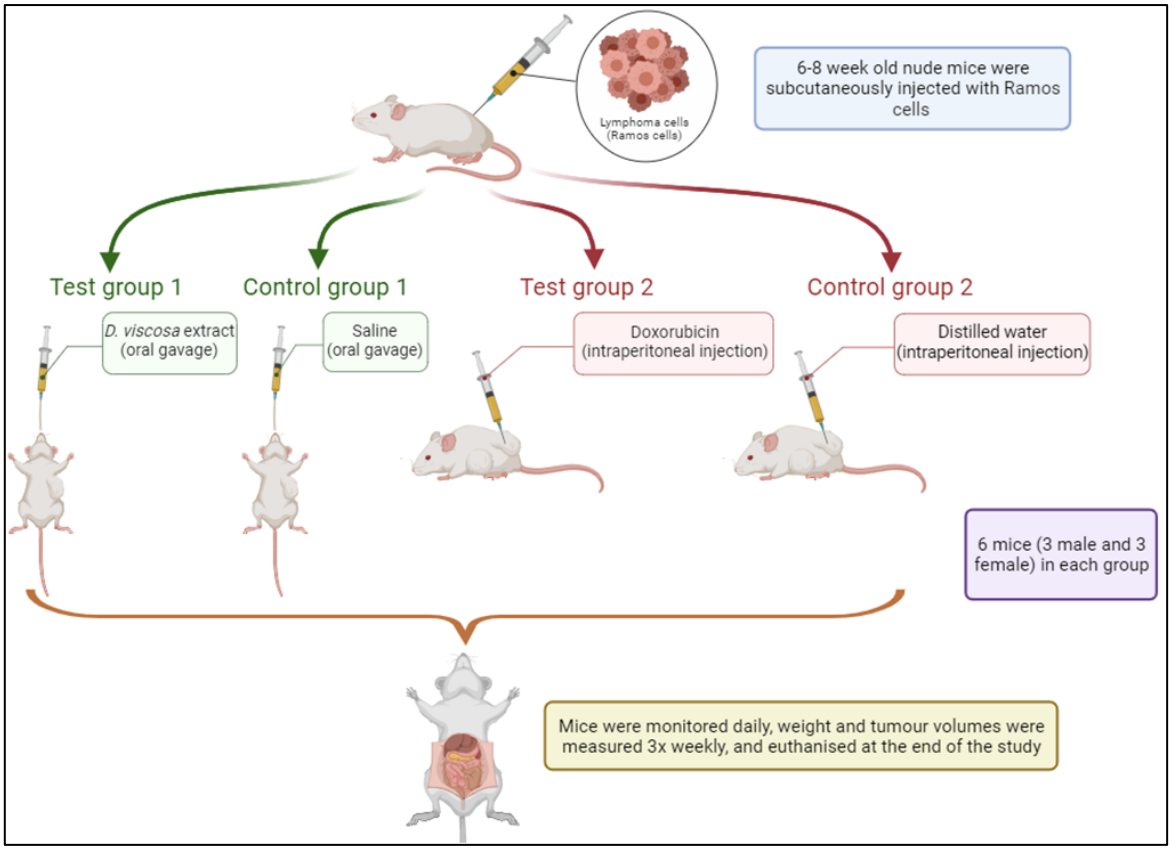


**Figure 3.12: Schematic diagram outlining the planned study using a BL xenograft mouse model to assess the effect of DVE on tumour formation.** Twenty four, 6-8 week old nude mice (12 m and 12 F) were subcutaneously injected in the hind flank with $1x10^7$ Ramos cells. Two weeks post-injection, mice were randomized into the four test groups of 6 mice each (3 M and 3 F). The mice in test group 1 received DVE (0.065 mg/g) daily via oral gavage and the control group 1 received the same volume of vehicle (saline). The mice in test group 2 received Doxorubicin (0.008mg/g) once a week via intraperitoneal injection and the control group 2 received the same volume of vehicle (distilled water). Welfare, weight, and tumour volume were monitored over time. At the study end point the mice were humanely euthanized. Created in Biorender.com.

### *3.3.3 DVE is less toxic than the chemotherapeutic drug Doxorubicin, and retards tumour growth.*

Fourteen days after the mice started receiving DVE / injected with Dox, the experiment was prematurely stopped due to a majority of the mice within the control groups having tumours which reached 2000 $mm^3$, the pre-defined experimental endpoint as per the recommendation of the Animal Ethics committee and ethical practice (Fig. 3.13).

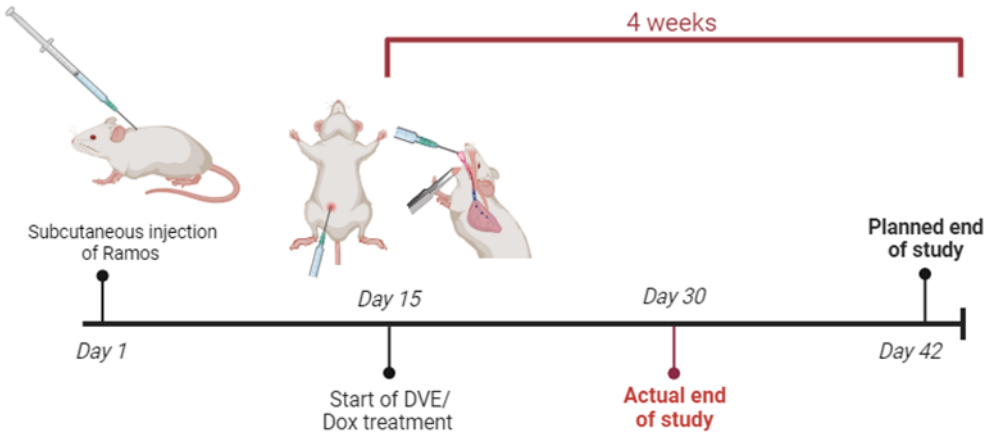


**Figure 3.13: Timeline of planned experiment, indicating points of premature and intended end of study.** 6-8 week old nude mice were subcutaneously injected, in the hind flank, with $1x10^7$ Ramos cells and tumour formation progressed for 2 weeks before DVE/DOX was administered. Planned and premature end of study are indicated.

Although data was collected for only half of the planned 4-week period, some interesting observations were made following data analysis. Mice who received DVE scored higher for body conditioning than mice who received Dox, indicating superior safety and tolerability of DVE compared to the therapeutic drug. This included consistent and sustained weight gain compared to the mice who received Dox (Fig. 3.14 A and B). Additionally, mice receiving DVE remained active and inquisitive, showed no signs of distress, were not pale and had good blood circulation to their extremities, while mice who received Dox had poor body condition scores and circulation, showed signs of distress and discomfort, became emaciated and pale in colour (representative mice are shown in Fig. 3.14 C and D; protruding spine shown by the red arrow). Interestingly, the majority of the tumours in the mice receiving DVE were very evidently necrotic, as can be seen by the red circle in Figure 3.14C, while the same was not observed for Dox-treated mice.

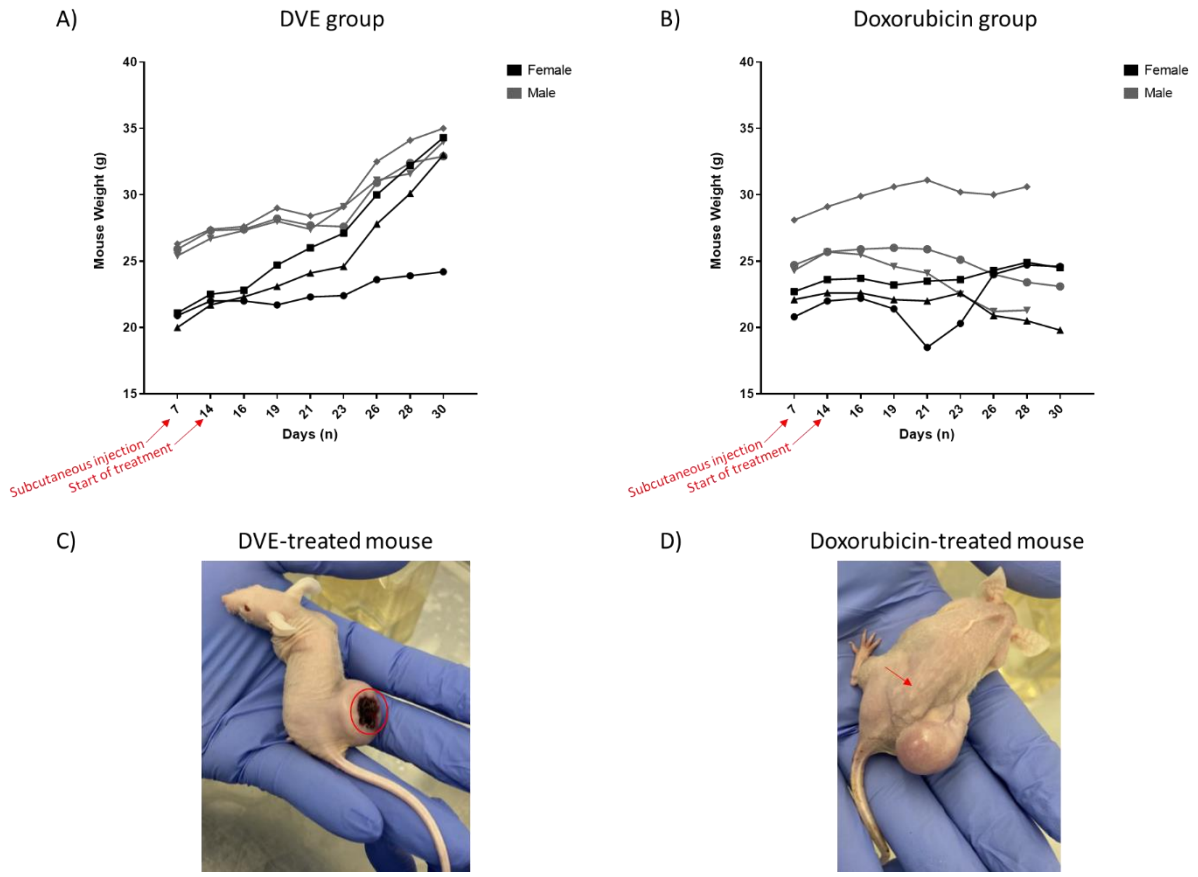


**Figure 3.14: *D. viscosa* extract is less toxic to nude mice compared to the chemotherapeutic drug, Doxorubicin**. Nude mice (6-8 weeks old) were subcutaneously injected in the hind flank with $1x10^7$ Ramos cells. Treatment commenced two-weeks post subcutaneous injection. The mice in the DVE test group (n = 6, 3 male and 3 female) received 0.065 mg/g DVE daily via oral gavage and the mice in the positive control test group (n = 6, 3 male and 3 female) received 0.008mg/g Doxorubicin once a week via intraperitoneal injection. The weights of the mice were recorded thrice a week. Data represents the weight of the male and female mice in the DVE-treated group (A) and the Doxorubicin-treated group (B). Data was analysed using GraphPad Prism 9 software. The images in C and D are representative of the effects of DVE (C) and Doxorubicin (D) treatment on the body conditions of the mice.

As per previous observation (section 3.4.1 above), tumours were more pronounced and developed faster in the male mice, compared to the female mice (Fig. 3.15). Despite the experiment being prematurely halted, the trend, specifically from day 26 until the experiment was stopped, shows that the tumours in the male mice receiving DVE were developing slower than the controls (receiving saline) within this group (Fig. 3.15 A). Similarly, as shown in Figure 3.15C, the average tumour volume in the DVE-treated male mice was much less than that of the control male mice, from day 26 onwards. A similar observation was not made for the female mice (Fig. 3.15B and C).

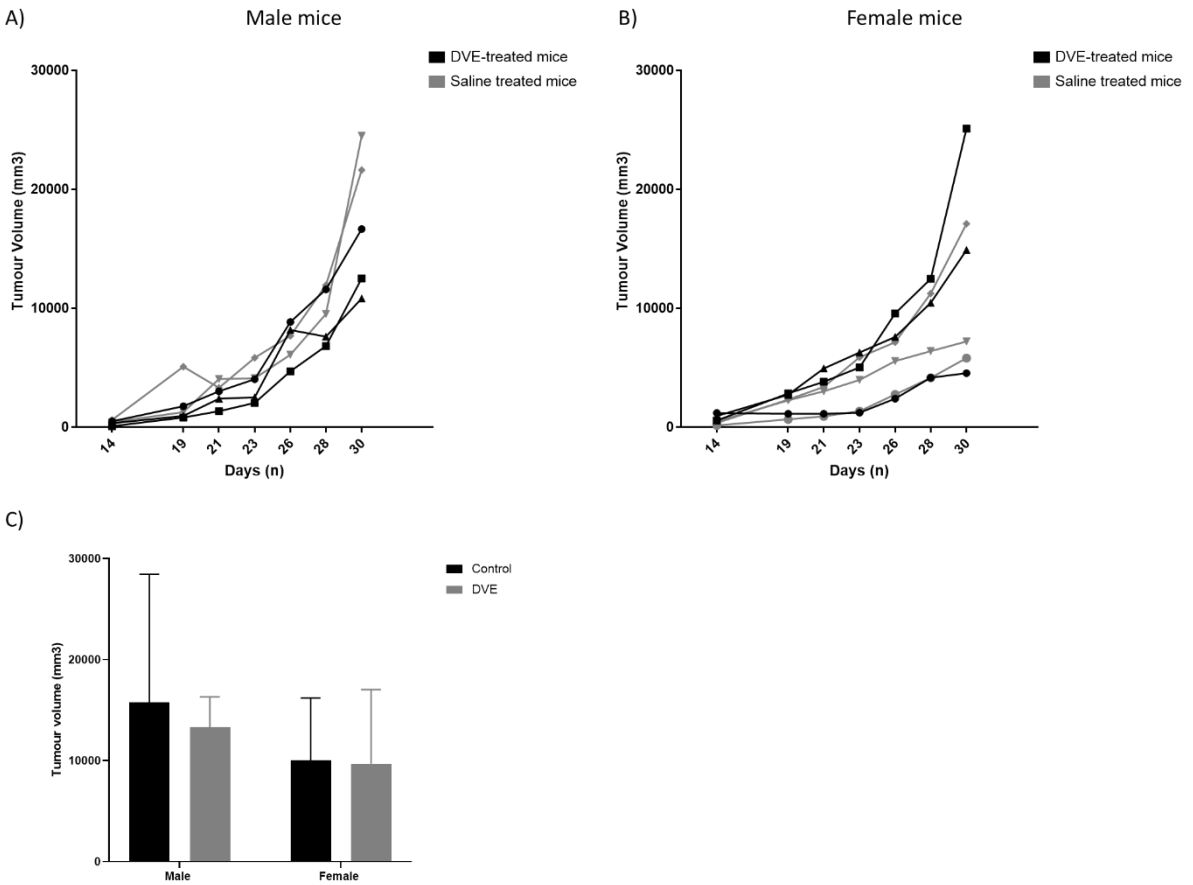


**Figure 3.15: *D. viscosa* extract slows down tumour growth as can be seen within the male nude mice groups.** Nude mice (6-8 weeks old) were subcutaneously injected in the hind flank with $1x10^7$ Ramos cells. Treatment commenced on day 14 and tumour size was measured thrice a week using venier calipers. Tumour volume was calculated using the following equation: *tumour volume ($mm^3$) = (length X width X width)/2.* The mice in the DVE test group (n = 6, 3 male and 3 female) received 0.065 mg/g DVE daily via oral gavage and its control arm received the equivalent volume of saline (vehicle). Due to tumour-formation failure in mouse #1 (from Control group), this mouse was excluded. The data represents the tumour volume of the male (A) and female (B) mice in the DVE-treated and control group. (C) Represents the average tumour volume of male and female mice in the DVE-treated and control group at the end of the experiment. Data was analysed using GraphPad Prism 9 software.

As mentioned above, tumours developed slower in the female mice, compared to the male mice, and this is most evident in the Doxorubicin control group (Fig. 3.16).

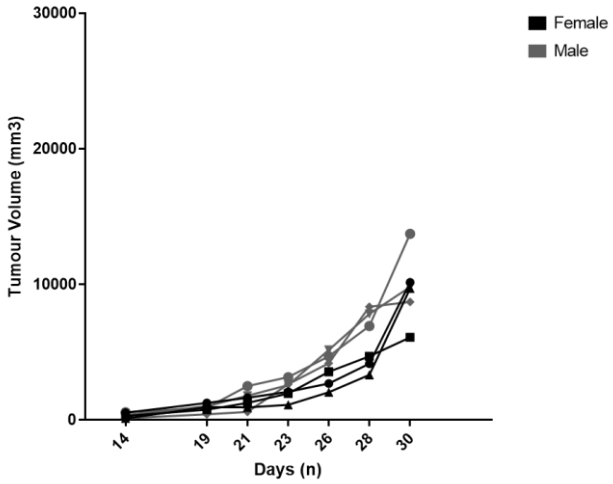


**Figure 3.16: Differences in tumour growth between male and female nude mice.** Nude mice (6-8 weeks old) were subcutaneously injected in the hind flank with $1x10^7$ Ramos cells. Treatment commenced on day 14 and tumour size was measured thrice a week using venier calipers. Tumour volume was calculated using the following equation: *tumour volume ($mm^3$) = (length X width X width)/2.* The mice in the Doxorubicin control test group (n = 6, 3 male and 3 female) received distilled water once a week via intraperitoneal injection. The data represents the tumour volume of the male and female mice in the Dox control group. Data was analysed using GraphPad Prism 9 software.

# Chapter 4: Discussion and Conclusion

In South Africa, traditional medical practitioners (TMP) are prevalent providers of alternative therapies and play an important part in the health care system due to their cultural role, availability, and accessibility. Additionally, many rural communities rely on TMPs as primary health care providers (Moshabela et al., 2015; Mothibe and Sibanda, 2016; Pinkoane et al., 2012; Street et al., 2018). Published reports indicate that up to 40% of cancer patients use at least one form of complementary and alternative medicine during their cancer treatment, and that this is due to a variety of reasons, including to alleviate the negative side effects associated with chemotherapy (Balneaves et al., 2022; Eng et al., 2003; Judson et al., 2016; Yates et al., 2005). Additionally, it is reported that, on average, 51% of cancer patients use alternative medicine as a form of cancer treatment. Since these medicines have not been appropriately tested and are not approved for use by the relevant regulatory bodies, they may potentially pose further health risks to these patients. (Judson et al., 2016). It is therefore important that the therapeutic utility of alternative therapies is scientifically and clinically assessed such that they can be safely and effectively incorporated into conventional therapy (Hamed et al., 2019; Hashem et al., 2022; Lin et al., 2020). Additionally, natural products and their bioactive compounds have been used for many years as structural models in the development of novel drugs, and several currently in-use chemo-preventative agents were originally derived from natural products. For example, the common chemotherapeutic drug, vincristine, is a vinca alkaloid isolated from the medicinal plant *Catharanthus roseus* – this plant is used by traditional healers for the treatment of diabetes, heart disease and cancer (Dhyani et al., 2022; Škubník et al., 2021). Another example is indole alkaloids derived from *Catharanthus roseus* used in the pharmaceutical industry for the treatment of various cancers including non-Hodgkin lymphoma, breast cancer and neuroblastoma (Dhyani et al., 2022; Hashem et al., 2022; Škubník et al., 2021)

*Dodonae viscosa* var. angustifolia is commonly used as a medicinal plant by the Rastafari Bush doctors, a group of traditional healers in the Western Cape region of South Africa. Although preliminary reports indicate that extracts from *D. viscosa* may have anti-proliferative and cytotoxic effects in breast, colon, cervical, and ovarian cancers, there are, to date, no comprehensive scientific reports that have used *in vitro* and *in vivo* assays to demonstrate the cytotoxic effects and therapeutic benefits of DVE in cancer (Al-Musawi and Al-Saadi, 2021; Herrera-Calderon et al., 2020; Jayaraman et al., 2021; Mossa and Al-Shawi, 2015; Palanisamy et al., 2021; Ramkumar et al., 2021)

There is no published research, to the best of our knowledge, on the anti-cancer properties of extracts of *D. viscosa* in aggressive lymphomas, including Burkitt lymphoma (BL), an HIV-associated cancer of high prevalence among people infected with HIV. The current standard treatment for BL includes

intensive high dose combination chemotherapy, that requires comprehensive supportive care, with 34% of patients achieving a 5-year overall survival (OS) and majority of patients experiencing relapsed/refractory disease (Opie et al., 2019; Zayac and Olszewski, 2020). There is therefore a need to identify novel chemotherapeutic agents, which would be more effective and have minimal off-target effects, particularly for the treatment of BL.

The results of this study provide evidence to show that aqueous extracts of *D. viscosa* (DVE) can potently and selectively inhibit the growth of Burkitt lymphoma cells and constitutes novel data since this has not been previously reported. DVE significantly inhibited the viability of two BL cell lines, namely Ramos and BL41, while having a significantly reduced effect on a non-cancerous lymphoblastoid cell line, with very favourable selectivity indices (Fig. 3.1). This is an important characteristic to consider during drug development, since a favourable selectivity index significantly decreases the likelihood of severe and undesirable side-effects during therapy, which then translates into improved overall outcome and quality of life for patients (Hashem et al., 2022; Lin et al., 2020).

Ethanolic extracts from the roots of *Dodonaea viscosa* (L.) Jacq. (Sapindaceae) (from the Madagascar rainforests) has been shown to inhibit the proliferation in ovarian cancer cells (A2780), as reported by Cao et al. (2009), with an $IC_{50}$ of 0.006 mg/ml. (Cao et al., 2009) Additionally, Mossa and Al-Shawi, (2015) reported an $IC_{50}$ of 0.075 mg/ml on breast cancer cells MDA-MB231, using ethanolic extract from *D. viscose* leaves collected from a province in Iraq (Mossa and Al-Shawi, 2015). The DVE $IC_{50}$ values we have reported in the current study, for both BL cell lines, are within range of these previously reported DVE $IC_{50}$ values, even though the plants are from very different geographical locations, and the extracts were prepared differently. The choice of solvent is an important step in the extraction process from plants, with alcoholic solvents, such as ethanol and methanol, being the most popular. However, these solvents have drawbacks, for instance, they can be unsuitable for certain uses in medicine. The use of purified water to prepare aqueous extracts is safer for downstream applications, and thus this method was chosen in the current research, in addition to the fact that traditional healers administer herbal preparations which, in the majority of cases, are non-ethanolic. However, it is important to note that the composition of biologically active compounds within an ethanolic versus an aqueous extract will differ.

Interestingly, in our study, DVE displayed more potent effects on the Ramos cell line ($IC_{50}$ value of 0.06 mg/ml) compared to BL41 ($IC_{50}$ value of 0.18 mg/ml). This type of differential response is not uncommon and could be attributed to the genetic profile of the respective cell lines. Most cancers are genetically heterogeneous in nature, and BL is no exception. In the two cell lines used in the study, it is likely that different cellular pathways mediate the responses to DVE treatment. A study by Panea et

al (2019) performed whole genome sequencing on 101 BL tumour samples and identified mutations in coding and non-coding regions of 72 driver genes (Panea et al., 2019). These genes have functions in cellular signalling, metabolic and DNA repair pathways, such as the PI3K, MAPK, cell cycle and tonic BCR signalling pathways. This heterogeneity explains the variability in treatment response, as well as relapse rates observed during treatment of patients (King et al., 2022; Panea et al., 2019; Schmitz et al., 2012). Although both the Ramos and the BL41 cell lines were originally derived from Caucasian male patients, each have distinct mutation profiles. Ramos has been reported to aberrantly express various c-MYC interacting proteins such as the oncogene BCL6 and tumour suppressor proteins PARP10 and SMARCA4 (Cardenas et al., 2017; Rouillard et al., 2016; Schleicher et al., 2018). Furthermore, the Ramos cell line has been reported to have mutated TCF3, a transcription factor which has been demonstrated by several studies to be aberrantly expressed in ~70% of BL cases (Crombie and LaCasce, 2021). Contrastingly, BL41 cells have been shown to differentially express several MAPK proteins, namely MAP3K1, MAP3K14, MAP3K4, MAP4K4, MAPKAPK3 and MAPKBP1, which have been reported to have both oncogenic and tumour suppressor roles (Avivar-Valderas et al., 2018; Gonzalez-Montero et al., 2023). Additionally, key regulatory proteins in the PI3K/mTOR pathway such as PIK3C2G, PIK3C3 and mTOR are also aberrantly expressed in BL41. It is therefore likely that the differential response is a result of different cellular pathways contributing to lymphomagenesis in these cell lines.

One of the characteristic hallmark traits of cancer cells is their ability to sustain proliferative signalling by either deregulating growth factor signals and pathways, or inducing oncogenic mutations which disrupts negative feedback mechanisms that diminish proliferative signalling (Hanahan and Weinberg, 2011). In this study DVE was shown to negatively impact the proliferation of BL cells. This was shown using colony formation (Fig. 3.2), as well as a proliferation tracking assays (Fig. 3.3). The negative impact on proliferation was relatively mild, as observed in the Cell Trace assay (10.5% for Ramos cells and 17.6% for BL41 cells), compared to effects observed on induction of apoptosis. It has to be noted however that, for the Cell Trace experiment, half of the $IC_{50}$ DVE concentration was used, over a period of 48 hours. This was done to ensure that an impact on proliferation could be measured, as opposed to apoptosis.

The induction of apoptosis by DVE, in the BL cells, was much more potent, than its impact on cell proliferation. This was demonstrated through multiples analyses, namely, impact on cell morphology (Fig. 3.4); incorporation of Annexin V (Fig. 3.5); activity of Caspase 3/7 enzymes (Fig. 3.6), and the expression of effector apoptotic-mediating proteins (Fig. 3.7). The three major and most well described modes of cell death are apoptosis, necrosis, and autophagy. Apoptosis is the preferred mode of cell death by chemotherapeutic agents as it is a programmed process of cellular dismantling that avoids eliciting inflammation as opposed to necrosis, while autophagy may be protective rather than

destructive to the cell (Liu and Jiao, 2020; Ouyang et al., 2012; Woo et al., 2020). Microscopy analyses revealed that both cell lines harboured morphological features typical of cells undergoing apoptosis when subjected to DVE treatment, such as clustering, swelling, membrane blebbing and nuclear dissolution. Furthermore, both cell lines displayed loss of plasma membrane asymmetry and integrity, as shown by Annexin V and propidium iodide incorporation. Notably, the BL41 cells were more susceptible (~20-fold increase in early apoptotic cells and a ~12-fold increase in late apoptotic cells) compared to Ramos cells (~8-fold increase in early apoptotic cells and a ~5-fold increase in late apoptotic cells), while the non-cancerous lymphoblastoid cells were mostly unaffected (Fig. 3.5). The expressions of the executioner caspase 3, and its substrate, cleaved PARP, were potently upregulated in BL cells subjected to DVE treatment, while this was not observed in the LCLs (Fig. 3.6). A relatively large variability in the activities of the caspase 3 and 7 enzymes was observed in BL41 cells following DVE treatment. This could be due to the fact that a majority of the cells were undergoing late apoptosis (55.7%), as observed in the Annexin V assay. At this advanced stage of apoptosis, caspase activity would be unstable or would have ceased due to the dismantling of the cell organelles and the degradation of nucleic acids and proteins.

It is worth mentioning that, over the duration of the research project, it became evident that the potency of batches of DVE varied, with decreased potency observed over time. While the lyophilized DVE powder used throughout the study was from the same harvest batch, DVE powder was prepared at approximately ±18 months intervals using frozen plant material. The stock solution prepared most recently was less potent than that which was prepared at the start of the research, inferring that the DVE lyophilized powder lost potency over time (Appendix A). Therefore, it cannot be deduced with certainty that Ramos and BL41 cells are differentially affected by DVE, since this may have been as a result of a more, or less potent, DVE used at the time of the assay. Nevertheless, DVE always displayed significantly more cytotoxicity towards the BL cancers cells relative to the non-cancerous LCLs at any point in time. The unstable nature of the *D. viscosa* extract signifies the importance of identifying the bioactive compounds and using those as lead compounds to develop more stable versions through structural modifications. With the assistance of chemists, this work has started, whereby high-performance liquid chromatography has been used to isolate four candidate compounds from DVE which will be tested in cytotoxicity assays against BL cells.

The identification of the signalling pathways affected by a drug candidate is crucial to the study of the mechanisms of drug action, toxicity and for repurposing (Hashem at al., 2022; Lin et al.,2020). The PI3K/AKT/mTOR signalling pathway plays a critical role in regulating important biological activities such as cellular proliferation, growth, survival, and metabolism (Noorolyai et al., 2019). This pathway is activated through the binding of growth factors/cytokines/hormones to various transmembrane

receptors (receptor tyrosine kinases, G-protein coupled receptors, toll-like receptors, and B-cell receptors). Upon stimulation, PI3K is recruited to the cell membrane and becomes allosterically activated thereby initiating the pathway's signalling cascade (He et al., 2021; Shi et al., 2019). In many cancers, these transmembrane receptors are constitutively activated independent of ligand binding. In particular, the development of B-cell lymphomagenesis is a result of tonic B-cell receptor (BCR) signalling, independent of ligand binding (Zayac and Olszewsk, 2020). Additionally, genomic, and functional studies have recently reported that recurrent somatic mutations in TCF3 and ID3 result in an increase in tonic BCR signalling and constitutive activation of PI3K-AKT activity. Further evidence of the involvement of PI3K signalling in BL pathogenesis was depicted by Sander et al. (2012), who reported that transgenic mice engineered to overexpress MYC and constitutively active PI3K signalling in germinal center B cells developed tumours that histologically and genetically resemble BL (Sander et al., 2012). This is supported by Schmitz et al. (2012), using high throughput RNA sequencing, which demonstrates that continuous PI3K activation is a consistent characteristic of BL tumours. In this study, the cytotoxic action of DVE was demonstrated to be via the alteration of key components of the PI3K/AKT pathway (Fig. 3.9 and 3.10). This is evident in both Ramos and BL41 cell lines whereby DVE led to enhanced expression of p-PTEN, a prime antagonist of PI3K. Inactivating mutations and loss of p-PTEN has been demonstrated in many cancers – compromised PTEN expression leads to $PIP_3$ accumulation and uncontrolled activation of AKT (Noorolyai et al., 2019). Conversely, overexpression of PTEN has been shown to inhibit proliferation and to induce apoptosis in Burkitt lymphoma cell lines, Raju and CA46 (Li et al., 2020). As yet, the status of p-PTEN in both Ramos and BL41 is not known, but the protein has been reported as detectable in these cell lines (Gehringer et al., 2020).

As a consequence of PTEN downregulation upon DVE treatment, the expression of downstream kinase p-PDK1 was significantly downregulated in the Ramos cells, which in turn infers that AKT phosphorylation is impaired. Indeed, no p-AKT(Ser 473) was detectable, and in fact, the level of total AKT increased, since the latter was not being processed to its active phosphorylated form. The expression of activated GSK3β, the downstream substrate of activated AKT, was upregulated in Ramos cells.

In the BL41 cell line, the observations were slightly different. Treatment with DVE led to a comparatively mild upregulation of activated p-PDK1, and a significant increase in both p-AKT(Ser 473) and p-GSK3β. This infers that the canonical PI3K pathway plays a more significant role in DVE-mediated cytotoxicity in Ramos cells than it does in BL41.

Although p-GSK3β was noted to be upregulated in both cell lines, it is important to note that this factor has been reported to function both as a tumour promoter and a tumour suppressor. The GSK3 family

consists of two isoforms, namely GSK3α and GSK3β, reported to have distinct functions in the regulation of cellular proliferation, differentiation, apoptosis, motility, and the cell cycle, and to mediate a number of cellular pathways including the PI3K/AKT; MAPK; NF-κB and WNT/β-catenin pathways (Duda et al., 2020). In the PI3K pathway, GSK3β has been shown to be negatively regulated by AKT thereby inhibiting its modulation of various oncogenes such as c-MYC, cyclin D1 and β-catenin. Therefore, GSK3 has been extensively researched as a therapeutic target, but subsequently demonstrated to have dual roles as a tumour suppressor and promoter in numerous cancers (Duda et al., 2020; He et al., 2020). Our findings suggest that GSK3β functions as a tumour suppressor in Burkitt lymphoma since its expression is enhanced upon DVE treatment.

Taken together, these findings suggest that DVE induces its cytotoxic effects in Ramos and BL41 by inhibiting PI3K/AKT signalling, that this effect is more pronounced in the Ramos cells, and that a second pathway is likely involved in BL41. One of the beneficial properties of natural products is their ability to target multiple signalling pathways in cancer cells. This has been demonstrated extensively in previous reports – for instance, the natural compound quercetin has been shown to target the MAPK, NF-κB, PI3K/AKT and Raf/Ras pathways to induce apoptosis and inhibit proliferation in Burkitt lymphoma, Diffuse Large B-cell Lymphoma and Hodgkin lymphoma (Soofiyani et al., 2021). Additionally, curcumin was reported to inhibit the NF-κB and Wnt- β-catenin pathways and modulate the MAPK pathway in cancer cells (Sarkar et al., 2009).

The results of our *in vitro* studies led to pre-clinical studies in a xenograft mouse model. Administration of DVE retarded tumour growth in mice, an effect which was most evident in male mice. We believe that this was attributed to the high speed at which the tumours developed and grew in male versus female mice. This was evident in both the pilot and experimental studies. Notably, Horesh and Horowitz (2014) reported that male patients had a higher incidence rate of developing Non-Hodgkin lymphoma (NHL) compared to females. This may be due to the protective effect of the female hormone, estrogen, to lymphoma development. Additionally, several authors have reported that female patients displayed a better response to standard R-CHOP treatment with higher overall survival (Horesh and Horowitz, 2014). Another factor could be the fact that the Ramos cell line was derived from a male patient and may thus be responsive to male hormones.

Body weight and conditioning scores indicate that DVE was much less toxic to the animals relative to the approved chemotherapeutic drug Doxorubicin (Fig. 3.14). Additionally, mice showed no signs of distress during the 2-week treatment, even when tumours were large. Dox-treated mice had poor body condition scores, exhibited visible signs of distress/discomfort, and became emaciated. This demonstrates that DVE may be a good candidate as an alternative/adjunct treatment for BL patients

as the extracts displays minimal side effects. Due to the unexpectedly fast speed at which tumours grew, the experiment was halted prematurely to prevent unethical suffering of experimental animals. Currently, a modified and improved proposal is being developed to allow for the analysis of the impact of DVE on BL tumour development in a xenograft mouse model over a longer period of time, using more mice per group, and the result will be included upon publication of this work.

Previous published reports have identified at least three other herbal extracts and/or compounds derived from herbal extracts, which display cytotoxic activities on Burkitt lymphoma cells. Ethanolic extracts from *Inula viscosa*, a traditional herb from the Asinara Island (part of Italy), was shown to inhibit the viability and induce apoptosis of the BL cell line Raji, within the 10 – 30 ug/ml range, and gene expression analysis showed downregulation of several anti-apoptotic genes including *c-MYC*, *CCND1* and *BLC2L1* (Virids et al., 2020). Shikonin (SHK), an active compound from extracts of the Chinese herbal medicinal plant *Lithospermum erythrorhizon*, was shown to supress proliferation and induce caspase-dependent apoptosis of the BL cell lines Namalwa and Raji, at a concentration range of 250 – 1250 nM (Ni et al., 2018). Additionally, SHK was found to significantly inhibit c-MYC protein expression in these cells, which in turn led to downregulation of the c-MYC target microRNA miR-19a, as well as elements of the PI3K pathway. Quercetin, a flavonoid found in many fruits, flowers and vegetables, has also been shown to reduce c-MYC expression and inhibit the Pi3K pathway in BL cells, leading to apoptotic cell death, with a higher toxicity observed against EBV-negative BL cells (2A8 and Ramos), relative to EBV-positive BL cells (Raji and Akata), suggesting that the virus promotes resistance to therapy (Granato et al., 2016). In our study, both BL cell lines used do not harbour EBV, and it would be useful in future studies to assess whether DVE is less effective on EBV-positive BL cells, relative to EBV-negative ones.

To summarise, the findings of this study have demonstrated that extracts of the medicinal plant, *Dodonae viscosa*, which is commonly used by traditional healers in the Western Cape region of South Africa, is a valuable resource for anti-cancer bioactive compounds, particularly for use in the treatment of Burkitt lymphoma, but may be beneficial for other cancers, particularly in cancers driven by PI3K/AKT signalling. Future work will involve the use of pre-clinical models to assess the performance of the extract *in vivo*, by designing a study, guided by the lessons learnt from the *in vivo* study reported upon here. This includes inclusion of male mice only, increasing the sample size, and to begin treatment at an earlier time point post-subcutaneous infection of BL cells to start tumour formation. Additionally, bioactive compounds will be isolated and assessed for their anti-cancer properties using High-performance liquid chromatography.

# References


1. Annexin A5 affinity assay. 2016 Available: https://en.wikipedia.org/wiki/Annexin_A5_affinity_assay [2017 , April 12].
2. Abayomi, E. A., Somers, A., Grewal, R., Sissolak, G., Bassa, F., Maartens, D., Jacobs, P., Stefan, C., & Ayers, L. W. (2011). Impact of the HIV epidemic and Anti-Retroviral Treatment policy on lymphoma incidence and subtypes seen in the Western Cape of South Africa, 2002-2009: Preliminary findings of the Tygerberg Lymphoma Study Group. Transfusion and Apheresis Science, 44(2), 161–166. https://doi.org/10.1016/j.transci.2011.01.007
3. Abdela, J. (2019). Evaluation of *in vivo* Antidiarrheal Activities of Hydroalcoholic Leaf Extract of Dodonaea viscosa L.(Sapindaceae) in Swiss Albino Mice. Journal of Evidence-Based Integrative Medicine, 24, 1–10. https://doi.org/10.1177/2515690X19891952
4. Al-Musawi, Z. F. H., & Al-Saadi, N. H. M. (2021). Antitumor activities of biosynthesized silver nanoparticles using Dodonaea viscosa (L.) leaves extract. Basrah Journal of Agricultural Sciences, 34(2), 42–59. https://doi.org/10.37077/25200860.2021.34.2.04
5. Al-Snafi, P. D. A. E. (2017). A review on Dodonaea viscosa: A potential medicinal plant. IOSR Journal of Pharmacy (IOSRPHR), 07(02), 10–21. https://doi.org/10.9790/3013-0702011021
6. Anandan, M., Poorani, G., Boomi, P., Varunkumar, K., Anand, K., Chuturgoon, A. A., Saravanan, M., & Gurumallesh Prabu, H. (2019). Green synthesis of anisotropic silver nanoparticles from the aqueous leaf extract of Dodonaea viscosa with their antibacterial and anticancer activities. Process Biochemistry, 80(February), 80–88. https://doi.org/10.1016/j.procbio.2019.02.014
7. Atallah-Yunes, S. A., Murphy, D. J., & Noy, A. (2020). HIV-associated Burkitt lymphoma. The Lancet Haematology, 7(8), e594–e600. https://doi.org/10.1016/S2352-3026(20)30126-5
8. Aung, T. N., Qu, Z., Kortschak, R. D., & Adelson, D. L. (2017). Understanding the effectiveness of natural compound mixtures in cancer through their molecular mode of action. International Journal of Molecular Sciences, 18(3). https://doi.org/10.3390/ijms18030656
9. Avivar-Valderas, A., McEwen, R., Taheri-Ghahfarokhi, A., Carnevalli, L. S., Hardaker, E. L., Maresca, M., Hudson, K., Harrington, E. A., & Cruzalegui, F. (2018). Functional significance of co-occurring mutations in PIK3CA and MAP3K1 in breast cancer. Oncotarget, 9(30), 21444–21458. https://doi.org/10.18632/oncotarget.25118
10. Aykul, S., & Martinez-Hackert, E. (2016). Determination of half-maximal inhibitory concentration using biosensor-based protein interaction analysis. Analytical biochemistry, 508, 97–103. https://doi.org/10.1016/j.ab.2016.06.025
11. Baharuddin, P., Satar, N., Fakiruddin, K. S., Zakaria, N., Lim, M. N., Yusoff, N. M., Zakaria, Z., & Yahaya, B. H. (2016). Curcumin improves the efficacy of cisplatin by targeting cancer stem-like cells through p21 and cyclin D1-mediated tumour cell inhibition in non-small cell lung cancer cell lines. Oncology Reports, 35(1), 13–25. https://doi.org/10.3892/or.2015.4371
12. Bailey, R. W., Nguyen, T., Robertson, L., Gibbons, E., Nelson, J., Christensen, R. E., Bell, J. P., Judd, A. M., & Bell, J. D. (2009). Sequence of physical changes to the cell membrane during glucocorticoid-induced apoptosis in S49 lymphoma cells. Biophysical Journal, 96(7), 2709–2718. https://doi.org/10.1016/j.bpj.2008.12.3925
13. Balneaves, L. G., Watling, C. Z., Hayward, E. N., Ross, B., Taylor-Brown, J., Porcino, A., & Truant, T. L. O. (2022). Addressing Complementary and Alternative Medicine Use among Individuals with Cancer: An Integrative Review and Clinical Practice Guideline. Journal of the National Cancer Institute, 114(1), 25–37. https://doi.org/10.1093/jnci/djab048
14. Banfalvi, G. (2017). Methods to detect apoptotic cell death. Apoptosis, 22(2), 306–323. https://doi.org/10.1007/s10495-016-1333-3

15. Barnabas, R. V, Szpiro, A. A., van Rooyen, H., Asiimwe, S., Pillay, D., Ware, N. C., Schaafsma, T. T., Krows, M. L., van Heerden, A., Joseph, P., Shahmanesh, M., Wyatt, M. A., Sausi, K., Turyamureeba, B., Sithole, N., Morrison, S., Shapiro, A. E., Roberts, D. A., Thomas, K. K., … Celum, C. (2020). Community-based antiretroviral therapy versus standard clinic-based services for HIV in South Africa and Uganda (DO ART): a randomised trial. The Lancet Global Health, 8(10), e1305–e1315. https://doi.org/https://doi.org/10.1016/S2214-109X(20)30313-2
16. Bhatti, M., Ippolito, T., Mavis, C., Gu, J., Cairo, M. S., Lim, M. S., Hernandez-Ilizaliturri, F., & Barth, M. J. (2018). Pre-clinical activity of targeting the PI3K/Akt/mTOR pathway in Burkitt lymphoma. Oncotarget, 9(31), 21820–21830. https://doi.org/10.18632/oncotarget.25072
17. Bray, F. et al. (2018) 'Global cancer statistics 2018: GLOBOCAN estimates of incidence and mortality worldwide for 36 cancers in 185 countries.', CA: a cancer journal for clinicians, 68(6), pp. 394–424. doi: 10.3322/caac.21492.
18. Cardenas, M. G., Oswald, E., Yu, W., Xue, F., MacKerell, A. D., & Melnick, A. M. (2017). The expanding role of the BCL6 oncoprotein as a cancer therapeutic target. Clinical Cancer Research, 23(4), 885–893. https://doi.org/10.1158/1078-0432.CCR-16-2071
19. Cao, S., Brodie, P., Callmander, M., Randrianaivo, R., Rakotobe, E., Rasamison, V. E., Tendyke, K., Suh, E. M., & Kingston, D. G. I. (2009). NIH Public Access. 72(9), 1705–1707. https://doi.org/10.1021/np900293x.Antiproliferative
20. Carmona, S., Bor, J., Nattey, C., Maughan-Brown, B., Maskew, M., Fox, M. P., Glencross, D. K., Ford, N., & MacLeod, W. B. (2018). Persistent High Burden of Advanced HIV Disease Among Patients Seeking Care in South Africa's National HIV Program: Data From a Nationwide Laboratory Cohort. Clinical Infectious Diseases, 66(suppl_2), S111–S117. https://doi.org/10.1093/cid/ciy045
21. Coiffier B, Thieblemont C, Van Den Neste E, et al (2010) Long-term outcome of patients in the LNH-98.5 trial, the first randomized study comparing rituximab-CHOP to standard CHOP chemotherapy in DLBCL patients: a study by the Groupe d'Etudes des Lymphomes de'Adulte. Blood. 116(12):2040–2045
22. Crombie, J., & LaCasce, A. (2021). The treatment of Burkitt lymphoma in adults. Blood, 137(6), 743–750. https://doi.org/10.1182/blood.2019004099
23. De Roubaix M. (2016). The decolonialisation of medicine in South Africa: Threat or opportunity?. South African medical journal = Suid-Afrikaanse tydskrif vir geneeskunde, 106(2), 159–161. https://doi.org/10.7196/SAMJ.2016.v106i2.10371
24. Demchenko, A. P. (2013). Beyond annexin V: Fluorescence response of cellular membranes to apoptosis. Cytotechnology, 65(2), 157–172. https://doi.org/10.1007/s10616-012-9481-y
25. Dhyani, P., Quispe, C., Sharma, E., Bahukhandi, A., Sati, P., Attri, D. C., Szopa, A., Sharifi-Rad, J., Docea, A. O., Mardare, I., Calina, D., & Cho, W. C. (2022). Anticancer potential of alkaloids: a key emphasis to colchicine, vinblastine, vincristine, vindesine, vinorelbine and vincamine. Cancer Cell International, 22(1), 1–20. https://doi.org/10.1186/s12935-022-02624-9
26. Duda, P., Akula, S. M., Abrams, S. L., Steelman, L. S., Martelli, A. M., Cocco, L., Ratti, S., Candido, S., Libra, M., Montalto, G., Cervello, M., Gizak, A., Rakus, D., & McCubrey, J. A. (2020). Targeting GSK3 and Associated Signaling Pathways Involved in Cancer. Cells, 9(5). https://doi.org/10.3390/cells9051110
27. du Sert, N., Ahluwalia, A., Alam, S., Avey, M. T., Baker, M., Browne, W. J., Clark, A., Cuthill, I. C., Dirnagl, U., Emerson, M., Garner, P., Holgate, S. T., Howells, D. W., Hurst, V., Karp, N. A., Lazic, S. E., Lidster, K., MacCallum, C. J., Macleod, M., … Würbel, H. (2020). Reporting animal research: Explanation and elaboration for the ARRIVE guidelines 2.0. PLOS Biology, 18(7), 1–65. https://doi.org/10.1371/journal.pbio.3000411

28. Dunleavy, K., Little, R. F., & Wilson, W. H. (2016). Update on Burkitt Lymphoma. Hematology/Oncology Clinics of North America, 30(6), 1333–1343. https://doi.org/10.1016/j.hoc.2016.07.009
29. Eng, J., Ramsum, D., Verhoef, M., Guns, E., Davison, J. & Gallagher, R. (2003). A Population-Based Survey of Complementary and Alternative Medicine Use in Men Recently Diagnosed with Prostate Cancer. Integrative Cancer Therapies. 2(3):212-216. DOI: 10.1177/1534735403256207.
30. Fiandalo, M. V., & Kyprianou, N. (2012). Caspase control: protagonists of cancer cell apoptosis. Experimental oncology, 34(3), 165–175.
31. Freer, J., & Mudaly, V. (2022). HIV and covid-19 in South Africa. BMJ, 376. https://doi.org/10.1136/bmj-2021-069807
32. Freshney, R. (2010). Culture of Animal Cells: A Manual of Basic Technique and Specialized Applications, Sixth Edition. In Culture of Animal Cells: A Manual of Basic Techniques and Specialized Application (Vol. 346). https://doi.org/10.1002/9780470649367
33. Gehringer, F., Weissinger, S. E., Möller, P., Wirth, T., & Ushmorov, A. (2020). Physiological levels of the PTEN-PI3K-AKT axis activity are required for maintenance of Burkitt lymphoma. Leukemia, 34(3), 857–871. https://doi.org/10.1038/s41375-019-0628-0
34. Givan, A. L., Fisher, J. L., Waugh, M., Ernstoff, M. S., & Wallace, P. K. (1999). A flow cytometric method to estimate the precursor frequencies of cells proliferating in response to specific antigens. Journal of Immunological Methods, 230(1), 99–112. https://doi.org/https://doi.org/10.1016/S0022-1759(99)00136-2
35. González-Montero, J., Rojas, C. I., & Burotto, M. (2023). MAP4K4 and cancer: ready for the main stage? Frontiers in Oncology, 13(May), 1–5. https://doi.org/10.3389/fonc.2023.1162835
36. Granato, M., Rizzello, C., Romeo, M. A., Yadav, S., Santarelli, R., D'Orazi, G., Faggioni, A., & Cirone, M. (2016). Concomitant reduction of c-Myc expression and PI3K/AKT/mTOR signaling by quercetin induces a strong cytotoxic effect against Burkitt's lymphoma. International Journal of Biochemistry and Cell Biology, 79, 393–400. https://doi.org/10.1016/j.biocel.2016.09.006
37. Hamed Al Bimani, B. M., & Hossain, M. A. (2020). A new antimicrobial compound from the leaves of Dodonaea viscosa for infectious diseases. Bioactive Materials, 5(3), 602–610. https://doi.org/10.1016/j.bioactmat.2020.04.006
38. Hamed, A. R., Abdel-Azim, N. S., Shams, K. A., & Hammouda, F. M. (2019). Targeting multidrug resistance in cancer by natural chemosensitizers. Bulletin of the National Research Centre, 43(1). https://doi.org/10.1186/s42269-019-0043-8
39. Hämmerl, L., Colombet, M., Rochford, R., Ogwang, D. M., & Parkin, D. M. (2019). The burden of Burkitt lymphoma in Africa. Infectious Agents and Cancer, 14(1), 1–6. https://doi.org/10.1186/s13027-019-0236-7
40. Hammond, M., Kohn, J., Oh, K., Piatti, P., & Liu, N. (2020). A method for greater reliability in Western Blot loading controls: Stain-free total protein quantification. www.bio-rad.com. Retrieved May 1, 2023, from https://www.bio-rad.com/webroot/web/pdf/lsr/literature/Bulletin_6360.pdf
41. Hanahan, D., & Weinberg, R. A. (2011). Hallmarks of cancer: The next generation. Cell, 144(5), 646–674. https://doi.org/10.1016/j.cell.2011.02.013
42. Hashem, S., Ali, T. A., Akhtar, S., Nisar, S., Sageena, G., Ali, S., Al-Mannai, S., Therachiyil, L., Mir, R., Elfaki, I., Mir, M. M., Jamal, F., Masoodi, T., Uddin, S., Singh, M., Haris, M., Macha, M., & Bhat, A. A. (2022). Targeting cancer signalling pathways by natural products: Exploring promising anti-cancer agents. Biomedicine and Pharmacotherapy, 150, 113054. https://doi.org/10.1016/j.biopha.2022.113054

43. He, Y., Sun, M. M., Zhang, G. G., Yang, J., Chen, K. S., Xu, W. W., & Li, B. (2021). Targeting PI3K/Akt signal transduction for cancer therapy. Signal Transduction and Targeted Therapy, 6(1). https://doi.org/10.1038/s41392-021-00828-5
44. He, R., Du, S., Lei, T., Xie, X., & Wang, Y. (2020). Glycogen synthase kinase 3β in tumorigenesis and oncotherapy (Review). Oncology Reports, 44(6), 2373–2385. https://doi.org/10.3892/or.2020.7817
45. Herrera-Calderon, O., Rahman, M. H., Pena-Rojas, G., & Andia-Ayme, V. (2020). Dodonaea viscosa Jacq: A medicinal plant with cytotoxic effect on colon cancer cell line (HT-29). Journal of Pure and Applied Microbiology, 14(3), 1927–1934. https://doi.org/10.22207/JPAM.14.3.31
46. Hossain, M. A. (2019). Biological and phytochemicals review of Omani medicinal plant Dodonaea viscosa. Journal of King Saud University - Science, 31(4), 1089–1094. https://doi.org/10.1016/j.jksus.2018.09.012
47. Hosseinzadeh, L., Behravan, J., Mosaffa, F., Bahrami, G., Bahrami, A., & Karimi, G. (2011). Curcumin potentiates doxorubicin-induced apoptosis in H9c2 cardiac muscle cells through generation of reactive oxygen species. Food and Chemical Toxicology, 49(5), 1102–1109. https://doi.org/10.1016/j.fct.2011.01.021
48. Human Colony-Forming Unit (CFU) Assays Using MethoCultTM Technical Manual. (2019, March). STEMCELL Technologies. Retrieved May 1, 2023, from https://cdn.stemcell.com/media/files/manual/MA28404-Human_Colony_Forming_Unit_Assays_Using_MethoCult.pdf
49. Improved CFSE Alternatives for Cell Proliferation (6 February 2023) Thermo Fisher Scientific - US. Available at: https://www.thermofisher.com/za/en/home/life-science/cell-analysis/flow-cytometry/flow-cytometry-assays-reagents/cell-proliferation-flow-cytometry/improved-cfse-alternatives-cell-proliferation.html (Accessed: February 13, 2023)
50. Jayaraman, A., Karthikeyan, V., & Akilan, C. A. (2021). Antimicrobial , Antioxidant and Anticancerous Studies on Dodonaea viscosa Leaf Extracts Against Human Breast Cancer Cell Line ( MCF-7 ). 41, 468–480.
51. Jellusova, J., & Rickert, R. C. (2016). The PI3K pathway in B cell metabolism. Critical Reviews in Biochemistry and Molecular Biology, 51(5), 359–378. https://doi.org/10.1080/10409238.2016.1215288
52. Judson, P. L., Abdallah, R., Xiong, Y., Ebbert, J., & Lancaster, J. M. (2017). Complementary and Alternative Medicine Use in Individuals Presenting for Care at a Comprehensive Cancer Center. Integrative Cancer Therapies, 16(1), 96–103. https://doi.org/10.1177/1534735416660384
53. Jung J. (2014). Human tumor xenograft models for preclinical assessment of anticancer drug development. Toxicological research, 30(1), 1–5. https://doi.org/10.5487/TR.2014.30.1.001
54. Kalisz, K., Alessandrino, F., Beck, R., Smith, D., Kikano, E., Ramaiya, N. H., & Tirumani, S. H. (2019). An update on Burkitt lymphoma: a review of pathogenesis and multimodality imaging assessment of disease presentation, treatment response, and recurrence. Insights into Imaging, 10(1), 1–16. https://doi.org/10.1186/s13244-019-0733-7
55. Keene, M. R., Heslop, I. M., Sabesan, S. S., & Glass, B. D. (2019). Complementary and alternative medicine use in cancer: A systematic review. Complementary Therapies in Clinical Practice, 35(January), 33–47. https://doi.org/10.1016/j.ctcp.2019.01.004
56. King, R. L., Hsi, E. D., Chan, W. C., Piris, M. A., Cook, J. R., Scott, D. W., & Swerdlow, S. H. (2023). Diagnostic approaches and future directions in Burkitt lymphoma and high-grade B-cell lymphoma. Virchows Archiv, 482(1), 193–205. https://doi.org/10.1007/s00428-022-03404-6
57. Klanova, M., & Klener, P. (2020). BCL-2 proteins in pathogenesis and therapy of B-Cell Non-Hodgkin lymphomas. Cancers, 12(4), 1–21. https://doi.org/10.3390/cancers12040938

58. Kluska, M., & Woźniak, K. (2021). Natural polyphenols as modulators of etoposide anti-cancer activity. International Journal of Molecular Sciences, 22(12). https://doi.org/10.3390/ijms22126602
59. Knecht, K., Kinder, D., & Stockert, A. (2020). Biologically-Based Complementary and Alternative Medicine (CAM) Use in Cancer Patients: The Good, the Bad, the Misunderstood. Frontiers in Nutrition, 6(January), 1–7. https://doi.org/10.3389/fnut.2019.00196
60. Lašťovička, J., Rataj, M., & Bartůňková, J. (2016). Assessment of lymphocyte proliferation for diagnostic purpose: Comparison of CFSE staining, Ki-67 expression and 3H-thymidine incorporation. Human Immunology, 77(12), 1215–1222. https://doi.org/https://doi.org/10.1016/j.humimm.2016.08.012
61. Li, C., Xu, Y., Xin, P., Zheng, Y., & Zhu, X. (2020). Role and mechanism of PTEN in Burkitt's lymphoma. Oncology Reports, 43(2), 481–490. https://doi.org/10.3892/or.2020.7457
62. Li, A., Chen, H., Lin, M., Zhang, C., Tang, E., Peng, J., Wei, Q., Li, H., & Yin, L. (2015). PIK3C2G copy number is associated with clinical outcomes of colorectal cancer patients treated with oxaliplatin. International Journal of Clinical and Experimental Medicine, 8(1), 1137–1143.
63. Lin, S. R., Chang, C. H., Hsu, C. F., Tsai, M. J., Cheng, H., Leong, M. K., Sung, P. J., Chen, J. C., & Weng, C. F. (2020). Natural compounds as potential adjuvants to cancer therapy: Preclinical evidence. British Journal of Pharmacology, 177(6), 1409–1423. https://doi.org/10.1111/bph.14816
64. Liu, Z. G., & Jiao, D. (2020). Necroptosis, tumour necrosis and tumorigenesis. Cell Stress, 4(1), 1–8. https://doi.org/10.15698/cst2020.01.208
65. Majolo, F., de Oliveira Becker Delwing, L. K., Marmitt, D. J., Bustamante-Filho, I. C., & Goettert, M. I. (2019). Medicinal plants and bioactive natural compounds for cancer treatment: Important advances for drug discovery. Phytochemistry Letters, 31(April), 196–207. https://doi.org/10.1016/j.phytol.2019.04.003
66. Matesun, D. A., Mensah, K. B., Yamoah, P., Bangalee, V., & Padayachee, N. (n.d.). Adverse drug reactions associated with doxorubicin and epirubicin: A descriptive analysis from VigiBase. Journal of Oncology Pharmacy Practice, 0(0), 10781552221113578. https://doi.org/10.1177/10781552221113578
67. McIlwain, D. R., Berger, T., & Mak, T. W. (2013). Caspase functions in cell death and disease. Cold Spring Harbor Perspectives in Biology, 5(4), 1–28. https://doi.org/10.1101/cshperspect.a008656
68. Morgensztern, D., & McLeod, H. L. (2005). PI3K/Akt/mTOR pathway as a target for cancer therapy. Anti-Cancer Drugs, 16(8), 797–803. https://doi.org/10.1097/01.cad.0000173476.67239.3b
69. Moshabela, M., Zuma, T., & Gaede, B. (2015). Bridging the gap between biomedical and traditional health practitioners in South Africa. 83–92.
70. Mossa, G. D., & Al-Shawi, A. A. A. (2015). Induction of Apoptosis through S-Phase in Human Breast Cancer MDA-MB231 Cells by Ethanolic Extract of Dodonaea Viscose L.-an Iraqi Medicine Plant. Journal of Basrah Researches, 41(1), 119–129. https://www.researchgate.net/publication/312320366
71. Mothibe, M. E., & Sibanda, M. (2016). African Traditional Medicine: South African Perspective Mmamosheledi. Intech, i(tourism), 13. https://doi.org/http://dx.doi.org/10.5772/57353
72. Naidoo, R., Patel, M., Gulube, Z., & Fenyvesi, I. (2012). Inhibitory activity of Dodonaea viscosa var. angustifolia extract against Streptococcus mutans and its biofilm. Journal of Ethnopharmacology, 144(1), 171–174. https://doi.org/10.1016/j.jep.2012.08.045
73. Ngabaza, T., Johnson, M. M., Moeno, S., & Patel, M. (2017). Identification of 5,6,8-Trihydroxy-7-methoxy-2-(4-methoxyphenyl)-4H-chromen-4-one with antimicrobial activity from

Dodonaea viscosa var. angustifolia. South African Journal of Botany, 112, 48–53. https://doi.org/10.1016/j.sajb.2017.05.024

74. Ni, F., Huang, X., Chen, Z., Qian, W., & Tong, X. (2018). Shikonin exerts antitumor activity in Burkitt's lymphoma by inhibiting C-MYC and PI3K/AKT/mTOR pathway and acts synergistically with doxorubicin. Scientific Reports, 8(1), 1–10. https://doi.org/10.1038/s41598-018-21570-z
75. Noorolyai, S., Shajari, N., Baghbani, E., Sadreddini, S., & Baradaran, B. (2019). The relation between PI3K/AKT signalling pathway and cancer. Gene, 698(March), 120–128. https://doi.org/10.1016/j.gene.2019.02.076
76. Opie, J., Antel, K., Koller, A., & Novitzky, N. (2020). In the South African setting, HIV-associated Burkitt lymphoma is associated with frequent leukaemic presentation, complex cytogenetic karyotypes, and adverse clinical outcomes. Annals of Hematology, 99(3), 571–578. https://doi.org/10.1007/s00277-020-03908-8
77. Ouyang, L., Shi, Z., Zhao, S., Wang, F. T., Zhou, T. T., Liu, B., & Bao, J. K. (2012). Programmed cell death pathways in cancer: A review of apoptosis, autophagy and programmed necrosis. Cell Proliferation, 45(6), 487–498. https://doi.org/10.1111/j.1365-2184.2012.00845.x
78. Oyebode, O., Kandala, N. B., Chilton, P. J., & Lilford, R. J. (2016). Use of traditional medicine in middle-income countries: A WHO-SAGE study. Health Policy and Planning, 31(8), 984–991. https://doi.org/10.1093/heapol/czw022
79. Palanisamy, C. P., Cui, B., Zhang, H., Panagal, M., Paramasivam, S., Chinnaiyan, U., Jeyaraman, S., Murugesan, K., Rostagno, M., Sekar, V., & Natarajan, S. P. (2021). Anti-ovarian cancer potential of phytocompound and extract from South African medicinal plants and their role in the development of chemotherapeutic agents. American Journal of Cancer Research, 11(5), 1828–1844. http://www.ncbi.nlm.nih.gov/pubmed/34094656%0Ahttp://www.pubmedcentral.nih.gov/articlerender.fcgi?artid=PMC8167668
80. Panea, R. I., Love, C. L., Shingleton, J. R., Reddy, A., Bailey, J. A., Moormann, A. M., Otieno, J. A., Ong'echa, J. M., Oduor, C. I., Schroeder, K. M. S., Masalu, N., Chao, N. J., Agajanian, M., Major, M. B., Fedoriw, Y., Richards, K. L., Rymkiewicz, G., Miles, R. R., Alobeid, B., … Dave, S. S. (2019). The whole-genome landscape of Burkitt lymphoma subtypes. Blood, 134(19), 1598–1607. https://doi.org/10.1182/blood.2019001880
81. Parrish, A. B., Freel, C. D., & Kornbluth, S. (2013). Activation and Function. Cold Spring Harbor Perspectives in Biology, 5(6), a008672. http://www.ncbi.nlm.nih.gov/pubmed/23732469%0Ahttp://www.pubmedcentral.nih.gov/articlerender.fcgi?artid=PMC3660825
82. Patel, M., & Coogan, M. M. (2008). Antifungal activity of the plant Dodonaea viscosa var. angustifolia on Candida albicans from HIV-infected patients. Journal of Ethnopharmacology, 118(1), 173–176. https://doi.org/10.1016/j.jep.2008.03.009
83. PE Annexin V Apoptosis Detection Kit I. Available at: https://www.bdbiosciences.com/en-eu/products/reagents/flow-cytometry-reagents/research-reagents/panels-multicolor-cocktails-ruo/pe-annexin-v-apoptosis-detection-kit-i.559763 (Accessed: 01 August 2023).
84. Petersen, L. M., Moll, E. J., Cape, W., Town, C., Africa, S., Collins, R. A. Y. J., & Hockings, M. T. (2014). '" Bush Doctors and Wild Medicine "': The Scale of Trade in Cape Town ' s Informal Economy of Wild-Harvested Medicine and Traditional Healing. March 2013, 315–336. https://doi.org/10.1080/08941920.2013.861558
85. Philander, Lisa E. Aston; Makunga, Nokwanda P.; Esler, K. J. (2014) The Informal Trade of Medicinal Plants by Rastafari Bush Doctors in the Western Cape of South Africa 1 68, 303–315.
86. Phillips, L. and Opie, J. (2018) 'The utility of bone marrow sampling in the diagnosis and staging of lymphoma in South Africa', (October 2017), pp. 276–283. doi: 10.1111/ijlh.12782.

87. Pinkoane MG, Greeff M, Koen MP (2012) A model for the incorporation of the traditional healers into the national health care delivery system in South Africa. Afr J Tradit complement Altern Med 9(3). 12-18
88. Quah, B. J., & Parish, C. R. (2010). The use of carboxyfluorescein diacetate succinimidyl ester (CFSE) to monitor lymphocyte proliferation. Journal of visualized experiments : JoVE, (44), 2259. https://doi.org/10.3791/2259
89. Quah, B. J. C., & Parish, C. R. (2012). New and improved methods for measuring lymphocyte proliferation *in vitro* and *in vivo* using CFSE-like fluorescent dyes. Journal of Immunological Methods, 379(1), 1–14. https://doi.org/https://doi.org/10.1016/j.jim.2012.02.012
90. Ramamurthy, V., Rajeswari, D. M., Gowri, R., Vadivazhagi, M. K., Jayanthi, G., & Raveendran, A. S. (2013). Study of the Phytochemical Analysis and Antimicrobial Activity of Dodonaea Viscosa. J. Pure Appl. Zool. INTERNATIONAL JOURNAL OF PURE AND APPLIED ZOOLOGY, 1(2), 178–184.
91. Ramkumar, R., Periyasamy, S. K., Venkatraman, B. R., & Sekar, K. G. (2021). In-vitro Anti-Cancer and Anti-Inflammatory Screening of Dodonaea viscosa. Journal of Pharmaceutical Research International, 33, 186–192. https://doi.org/10.9734/jpri/2021/v33i39b32194
92. Rashed, K., Luo, M.-T., Zhang, L.-T., & Zheng, Y.-T. (2013). Dodonaea viscosa ( L .) extracts as anti human immunodeficiency virus type-1 ( HIV-1 ) agents and phytoconstituents. Peak Journal of Medicinal Plant Research, 1(3), 19–24. https://www.peakjournals.org/sub-journals-PJMPR.html
93. Reagan-Shaw, S., Nihal, M., & Ahmad, N. (2007). Dose translation from animal to human studies revisited. The FASEB Journal, 22(3), 659–661. https://doi.org/10.1096/fj.07-9574lsf
94. Roche. (2007). Cell Proliferation Reagent WST-1. Cell Proliferation, 1(11), 1–4.
95. Rohde, M., Bonn, B. R., Zimmermann, M., Lange, J., Möricke, A., Klapper, W., Oschlies, I., Szczepanowski, M., Nage, I., Schrappe, M., Loeffler, M., Siebert, R., Reiter, A., & Burkhardt, B. (2017). Relevance of ID3-TCF3-CCND3 pathway mutations in paediatric aggressive B-cell lymphoma treated according to the non-Hodgkin lymphoma Berlin-Frankfurt-münster protocols. Haematologica, 102(6), 1091–1098. https://doi.org/10.3324/haematol.2016.156885
96. Rouillard, A. D., Gundersen, G. W., Fernandez, N. F., Wang, Z., Monteiro, C. D., & McDermott, M. G. (2016). The harmonizome: A collection of processed datasets gathered to serve and mine knowledge about genes and proteins. Database, 2016. https://doi.org/10.1093/database/baw100
97. Saleh, E. M., El-awady, R. A., Eissa, N. A., & Abdel-Rahman, W. M. (2012). Antagonism between curcumin and the topoisomerase II inhibitor etoposide: A study of DNA damage, cell cycle regulation and death pathways. Cancer Biology and Therapy, 13(11), 1058–1071. https://doi.org/10.4161/cbt.21078
98. Sánchez, B. G., Bort, A., Mateos-Gómez, P. A., Rodríguez-Henche, N., & Díaz-Laviada, I. (2019). Combination of the natural product capsaicin and docetaxel synergistically kills human prostate cancer cells through the metabolic regulator AMP-activated kinases. Cancer Cell International, 19(1), 1–14. https://doi.org/10.1186/s12935-019-0769-2
99. Sander, S., Calado, D. P., Srinivasan, L., Köchert, K., Zhang, B., Rosolowski, M., Rodig, S. J., Holzmann, K., Stilgenbauer, S., Siebert, R., Bullinger, L., & Rajewsky, K. (2012). Synergy between PI3K Signalling and MYC in Burkitt Lymphomagenesis. Cancer Cell, 22(2), 167–179. https://doi.org/10.1016/j.ccr.2012.06.012
100. Sander, S., & Rajewsky, K. (2012). Burkitt lymphomagenesis linked to MYC plus PI3K in germinal center B cells. Oncotarget, 3(10), 1066–1067. https://doi.org/10.18632/oncotarget.726
101. Satoh, M., Yasuda, T., Higaki, T., Goto, M., Tanuma, S., Ide, T., Furuichi, Y., & Sugimoto, M. (2003). Innate apoptosis of human B lymphoblasts transformed by Epstein-Barr virus:

modulation by cellular immortalization and senescence. Cell structure and function, 28(1), 61–70. https://doi.org/10.1247/csf.28.61
102. Savitskaya, M. A., & Onishchenko, G. E. (2015). Mechanisms of Apoptosis. Biochemistry. Biokhimiia, 80(11), 1393–1405. https://doi.org/10.1134/S0006297915110012
103. Schleicher, E. M., Galvan, A. M., Imamura-Kawasawa, Y., Moldovan, G. L., & Nicolae, C. M. (2018). PARP10 promotes cellular proliferation and tumorigenesis by alleviating replication stress. Nucleic Acids Research, 46(17), 8908–8916. https://doi.org/10.1093/nar/gky658
104. Schmitz, R., Young, R. M., Ceribelli, M., Jhavar, S., Xiao, W., Zhang, M., Wright, G., Shaffer, A. L., Hodson, D. J., Buras, E., Liu, X., Powell, J., Yang, Y., Xu, W., Zhao, H., Kohlhammer, H., Rosenwald, A., Kluin, P., Müller-Hermelink, H. K., … Staudt, L. M. (2012). Burkitt lymphoma pathogenesis and therapeutic targets from structural and functional genomics. Nature, 490(7418), 116–120. https://doi.org/10.1038/nature11378
105. Schmitz, R., Ceribelli, M., Pittaluga, S., Wright, G., & Staudt, L. M. (2014). Oncogenic mechanisms in Burkitt lymphoma. Cold Spring Harbor Perspectives in Medicine, 4(2), 1–13. https://doi.org/10.1101/cshperspect.a014282
106. Şen, Ö., Emanet, M., & Çulha, M. (2016). Chapter 3 – Biocompatibility evaluation of boron nitride nanotubes. In G. Ciofani & V. Mattoli (Eds.), Boron Nitride Nanotubes in Nanomedicine (pp. 41–58). William Andrew Publishing. https://doi.org/https://doi.org/10.1016/B978-0-323-38945-7.00003-1
107. Shalini, S., Dorstyn, L., Dawar, S., & Kumar, S. (2015). Old, new and emerging functions of caspases. Cell Death and Differentiation, 22(4), 526–539. https://doi.org/10.1038/cdd.2014.216
108. Sharifi-Rad, J., Ozleyen, A., Tumer, T. B., Adetunji, C. O., Omari, N. El, Balahbib, A., Taheri, Y., Bouyahya, A., Martorell, M., Martins, N., & Cho, W. C. (2019). Natural products and synthetic analogs as a source of antitumor drugs. In Biomolecules (Vol. 9, Issue 11). https://doi.org/10.3390/biom9110679
109. Shi, X., Wang, J., Lei, Y., Cong, C., Tan, D., & Zhou, X. (2019). Research progress on the PI3K/AKT signalling pathway in gynaecological cancer (Review). Molecular Medicine Reports, 19(6), 4529–4535. https://doi.org/10.3892/mmr.2019.10121
110. Škubník, J., Pavlíčková, V. S., Ruml, T., & Rimpelová, S. (2021). Vincristine in combination therapy of cancer: Emerging trends in clinics. Biology, 10(9). https://doi.org/10.3390/biology10090849
111. Soofiyani, S. R., Hosseini, K., Forouhandeh, H., Ghasemnejad, T., Tarhriz, V., Asgharian, P., Reiner, Ž., Sharifi-Rad, J., & Cho, W. C. (2021). Quercetin as a Novel Therapeutic Approach for Lymphoma. Oxidative Medicine and Cellular Longevity, 2021. https://doi.org/10.1155/2021/3157867
112. South African Cancer Statistics. (n.d.). CANSA. https://cansa.org.za/south-african-cancer-statistics/
113. Statistical release – statssa.gov.za (2022) Statistics South Africa. Available at: http://www.statssa.gov.za/publications/P0302/P03022021.pdf (Accessed: 24 May 2023).
114. Street, R. A., Smith, M., Moshabela, M., Shezi, B., Webster, C., & Falkenberg, T. (2018). Traditional health practitioners and sustainable development: a case study in South Africa. Public Health, 165, 1–5. https://doi.org/10.1016/j.puhe.2018.07.021
115. Success Story: Taxol. (n.d.). Success Story: Taxol. https://dtp.cancer.gov/timeline/flash/success_stories/s2_taxol.htm#:~:text=Paclitaxel%2C%20the%20most%20well%2Dknown,as%20well%20as%20Kaposi's%20sarcoma
116. Sung, H., Ferlay, J., Siegel, R. L., Laversanne, M., Soerjomataram, I., Jemal, A., & Bray, F. (2021). Global Cancer Statistics 2020: GLOBOCAN Estimates of Incidence and Mortality Worldwide for

36 Cancers in 185 Countries. CA: A Cancer Journal for Clinicians, 71(3), 209–249. https://doi.org/10.3322/caac.21660

117. Teffo, L. S., Aderogba, M. A., & Eloff, J. N. (2010). Antibacterial and antioxidant activities of four kaempferol methyl ethers isolated from Dodonaea viscosa Jacq. Var. angustifolia leaf extracts. South African Journal of Botany, 76(1), 25–29. https://doi.org/10.1016/j.sajb.2009.06.010The Global Cancer Observatory. (2020). Population Fact Sheets – South Africa. 491, 1–2. https://gco.iarc.fr/
118. Thirumaran, R., Prendergast, G. C., & Gilman, P. B. (2007). Chapter 7 – Cytotoxic Chemotherapy in Clinical Treatment of Cancer. In G. C. Prendergast & E. M. Jaffee (Eds.), Cancer Immunotherapy (pp. 101–116). Academic Press. https://doi.org/https://doi.org/10.1016/B978-012372551-6/50071-7
119. Tixeira, R., Caruso, S., Paone, S., Baxter, A. A., Atkin-Smith, G. K., Hulett, M. D., & Poon, I. K. H. (2017). Defining the morphologic features and products of cell disassembly during apoptosis. Apoptosis, 22(3), 475–477. https://doi.org/10.1007/s10495-017-1345-7
120. Turro, J., Singh, P., Sarao, M. S., Tadepalli, S., & Cheriyath, P. (2019). Adult Burkitt lymphoma-an Island between lymphomas and leukemias. Journal of Community Hospital Internal Medicine Perspectives, 9(1), 25–28. https://doi.org/10.1080/20009666.2019.1574545
121. Torre, L. A. et al. (2015) 'Global Cancer Statistics, 2012', CA: a cancer journal of clinicians., 65(2), pp. 87–108. Doi: 10.3322/caac.21262.
122. Ugwu, C. L. J., & Ncayiyana, J. R. (2022). Spatial disparities of HIV prevalence in South Africa. Do sociodemographic, behavioral, and biological factors explain this spatial variability? Frontiers in Public Health, 10. https://doi.org/10.3389/fpubh.2022.994277
123. Virdis, P., Migheli, R., Galleri, G., Fancello, S., Cadoni, M. P. L., Pintore, G., Petretto, G. L., Marchesi, I., Fiorentino, F. P., di Francesco, A., Sanges, F., Bagella, L., Muroni, M. R., Fozza, C., De Miglio, M. R., & Podda, L. (2020). Antiproliferative and proapoptotic effects of Inula viscosa extract on Burkitt lymphoma cell line. Tumor Biology, 42(2), 1–9. https://doi.org/10.1177/1010428319901061
124. Wallace, P. K., Tario Jr., J. D., Fisher, J. L., Wallace, S. S., Ernstoff, M. S., & Muirhead, K. A. (2008). Tracking antigen-driven responses by flow cytometry: Monitoring proliferation by dye dilution. Cytometry Part A, 73A(11), 1019–1034. https://doi.org/https://doi.org/10.1002/cyto.a.20619
125. Wang, C., Liu, J., & Liu, Y. (2022). Progress in the Treatment of HIV-Associated Lymphoma When Combined With the Antiretroviral Therapies. Frontiers in Oncology, 11(January), 1–7. https://doi.org/10.3389/fonc.2021.798008
126. Woo, Y., Lee, H. J., Jung, Y. M., & Jung, Y. J. (2020). Regulated Necrotic Cell Death in Alternative Tumour Therapeutic Strategies. Cells, 9(12), 1–17. https://doi.org/10.3390/cells9122709
127. Yang, Y. H., Mao, J. W., & Tan, X. L. (2020). Research progress on the source, production, and anti-cancer mechanisms of paclitaxel. Chinese Journal of Natural Medicines, 18(12), 10–17. https://doi.org/10.1016/S1875-5364(20)60032-2
128. Yates, J., Mustian, K., Morrow, G., Gillies, L., Padmanaban, D., Atkins, J., Issell, B. & Kirshner, J. et al. (2005). Prevalence of complementary and alternative medicine use in cancer patients during treatment. Supportive Care in Cancer. 13(10):806-811. DOI: 10.1007/s00520-004-0770-7.
129. Yuan, H. et al. (2016) 'The traditional medicine and modern medicine from natural products', Molecules, 21(5). Doi: 10.3390/molecules21050559.
130. Yuan TL; Cantley LC. (2008). PI3K pathway alterations in cancer. Oncogene, 27(41), 5497–5510. https://doi.org/10.1038/onc.2008.245.PI3K

131. Zayac, A. S., & Olszewski, A. J. (2020). Burkitt lymphoma: bridging the gap between advances in molecular biology and therapy. Leukemia and Lymphoma, 61(8), 1784–1796. https://doi.org/10.1080/10428194.2020.1747068
132. Zhang, X., Rakesh, K. P., Shantharam, C. S., Manukumar, H. M., Asiri, A. M., Marwani, H. M., & Qin, H. L. (2018). Podophyllotoxin derivatives as an excellent anticancer aspirant for future chemotherapy: A key current imminent needs. Bioorganic and Medicinal Chemistry, 26(2), 340–355. https://doi.org/10.1016/j.bmc.2017.11.026
133. Zhao, Q., Guan, J., Qin, Y., Ren, P., Zhang, Z., Lv, J., Sun, S., Zhang, C., & Mao, W. (2018). Curcumin sensitizes lymphoma cells to DNA damage agents through regulating Rad51-dependent homologous recombination. Biomedicine and Pharmacotherapy, 97(September 2017), 115–119. https://doi.org/10.1016/j.biopha.2017.09.078
134. Zheng, H. C. (2017). The molecular mechanisms of chemoresistance in cancers. Oncotarget, 8(35), 59950–59964. https://doi.org/10.18632/oncotarget.19048
135. Zhu, L., & Chen, L. (2019). Progress in research on paclitaxel and tumour immunotherapy. Cellular and Molecular Biology Letters, 24(1), 1–11. https://doi.org/10.1186/s11658-019-0164-y

# Appendix A

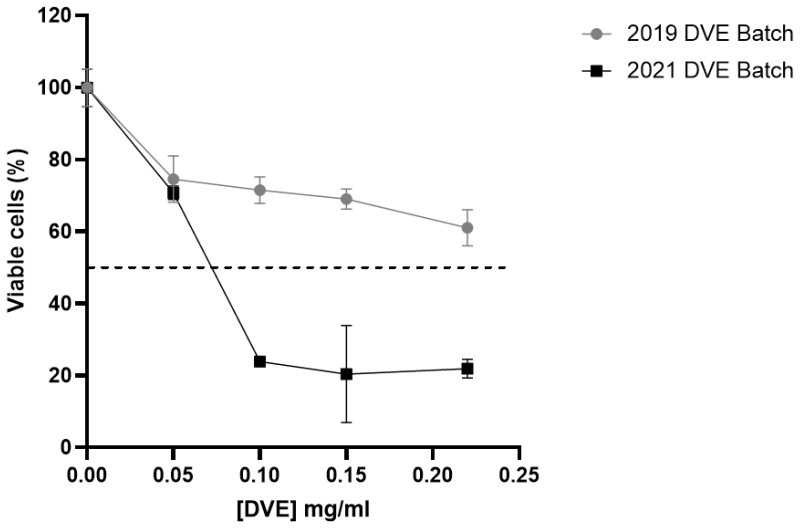


**Figure A1: Comparison of the cytotoxic effects of DVE batches prepared at different time points, on BL41.** Analysis was performed on an older batch of DVE (prepared in 2019) and freshly prepared batch (prepared in 2021). BL41 cells were treated with increasing concentrations of DVE (0.08 mg/ml – 0.3 mg/ml) and cell viability was measured after 24hrs of treatment, using the WST-1 assay. Data represents the mean ± Standard Deviation (N=3) for each concentration.

## Research output by candidate during the research period

1. Saferdien A and Mowla S. Investigating the anti-cancer properties of Dodonaea viscosa, a medicinal plant used by Cape Bush doctors. Annual Departmental Seminars. University of Cape Town. Oral presentation
2. Saferdien A and Mowla S. Investigating the anti-cancer properties of Dodonaea viscosa, a medicinal plant used by Cape Bush doctors. 13th Early Career Scientist Convention, South African Medical Research Council. 9th – 11th October 2019. Cape Town, South Africa. E-poster presentation
3. Saferdien A and Mowla S. Investigating the anti-cancer effects of Dodonaea viscosa, a herbal medicine used by traditional healers. HUB/IBMS/Pathology postgraduate research day. 26 November 2019. University of Cape Town, South Africa. Oral presentation.
4. Saferdien A and Mowla S. Investigating the anti-cancer effects of Dodonaea viscosa, a herbal medicine used by traditional healers. HUB/IBMS/Pathology biennial research symposium. 1 December 2021. University of Cape Town, South Africa E-poster presentation.
5. Saferdien A and Mowla S. Investigating the anti-cancer effects of Dodonaea viscosa, a herbal medicine used by traditional healers. 16th Early Career Scientist Convention, South African Medical Research Council. 25th – 26th October 2022. Cape Town, South Africa. Oral presentation
6. Saferdien A and Mowla S. Investigating the anti-cancer effects of *Dodonaea viscosa*, a herbal medicine used by traditional healers. South African Society for Biochemistry and Molecular Biology (SASBMB) virtual congress. 23rd -26th January 2022. Online. Oral presentation.
7. Saferdien A and Mowla S. Investigating the anti-cancer effects of Dodonaea viscosa, a herbal medicine used by traditional healers. 14th African Organisation for Research and Training in Cancer (AORTIC) International Conference on Cancer in Africa. 2nd – 6th November 2023. Dakar, Senegal. Poster presentation
8. Saferdien A and Mowla S. Investigating the anti-cancer effects of *Dodonaea viscosa*, a herbal medicine used by traditional healers. Research Capacity Development Beneficiary Conference, South African Medical Research Council. 20th – 21st November 2023. Cape Town, South African. Oral presentation.

# Appendix B

**UNIVERSITY OF CAPE TOWN**
**Faculty of Health Sciences**
**Animal Ethics Committee**

**Room G50 Old Main Building**
**Groote Schuur Hospital**
**Observatory 7925**
**Website:** www.health.uct.ac.za/fhs/research/animalethics/forms

30 November 2020

**Dr S. Mowla**
Division of Haematology
Department of Pathology
Faculty of Health Sciences
University of Cape Town

Dear Dr Mowla

**PROTOCOL TITLE:** Investigation of the anti-cancer properties of aqueous extracts from the medicinal plant Dodonaea viscosa using a mouse model (MSc Candidate: Ms Aaliyah Saferdien).

**FHS AEC REF NO: 019_038**

Thank you for submitting your amended protocol to the Faculty of Health Sciences (FHS) Animal Ethics Committee (AEC) for review.

I am pleased to inform you that the FHS AEC has **authorised** your protocol, which will terminate on **30 November 2023.**

Number of animals & species: 28 Nude Mice (UCT strain 21)

**Please quote the FHS AEC REF NO (above) in all future correspondence.**

Please note that the authorisation of this protocol imposes the following obligations on the principal investigator (PI):

1. To submit an annual mandatory progress report. The first annual report for this protocol is due on **28 February 2021**. The forms can be accessed from http://www.health.uct.ac.za/fhs/research/animalethics/forms
2. To submit a final mandatory report on the **30 November 2023**, please access the final report form from: http://www.health.uct.ac.za/fhs/research/animalethics/forms
3. Ensuring that all study participants perform within the confines of the procedures and experimental design of the protocol as authorised, or as amended.

4. Ensuring that all study participants comply with all applicable national legislation, UCT policies, FHS AEC policies and standard operating procedures (SOPs) and national standards (SANS 10386: 2008).
5. Ensuring compliance with DAFF Section 20 requirements.
6. Ensuring that you as the PI immediately alert the FHS AEC to any event involving the welfare of the animals which has occurred during the course of the study, as well as the actions that were taken to respond to these events.
7. Ensuring that you as the PI alert the FHS AEC to any new or unexpected ethical issues that arose during the course of the study, and how these issues were addressed.
8. Ensuring that all study participants are registered with or have been authorised by the South African Veterinary Council (SAVC) to perform the procedures on animals or will be performing the procedures under the direct and continuous supervision of SAVC-registered veterinary professionals or SAVC-registered para-veterinary professionals.
9. If the PI or any study participant is in any way uncertain how to respond to any of these obligations or deal with any of the issues referred to above, they must consult with FHS AEC.
10. All animals found dead must be reported to the RAF on the appropriate form: http://www.health.uct.ac.za/fhs/research/animalethics/forms
11. All animals found in distress must be reported to the RAF on the appropriate form.

My best wishes for a successful research and /or teaching endeavour.

Yours sincerely

**PROF G. LOUW**
**CHAIR, FHS AEC**

**AEC REF# 019_038**

# Appendix C

## Recipes and Reagents

### Tissue culture

**Supplemented growth media (making up 50 ml)**

| Cell Line | P/S | FBS | Medium |
|---|---|---|---|
| **L1439A** | 0.5 mL (1%) | 10 mL (20%) | 39.5 mL (DMEM) |
| **Ramos** | 0.5 mL (1%) | 5 mL (10%) | 44.5 mL (RPMI-1640) |
| **BL41** | 0.5 mL (1%) | 5 mL (10%) | 44.5 mL (RPMI-1640) |

Media was prepared under sterile conditions and stored at 4°C.

**Freezing Media**

| Cell Line | FBS | Cryo Preservative Agent | Medium |
|---|---|---|---|
| **L1439A** | 20% | Glycerol (10%) | DMEM (as needed) |
| **Ramos** | 10% | DMSO (10%) | RPMI (as needed) |
| **BL41** | 10% | DMSO (10%) | RPMI (as needed) |

Media was prepared on ice.

**10x PBS**

| | Weight (g) |
|---|---|
| **NaCl** | 80 g |
| **KCl** | 2 g |
| **$Na_2HPO_4$** | 14.4 g |
| **$KH_2PO_4$** | 2.4 g |

Dissolve in 800 ml $dH_2O$.
Adjust pH to 7.4 with HCl.
Fill up to 1L with $dH_2O$.
Autoclave and store at 4°C.

**1x PBS**

1:10 dilution of 10x PBS with $dH_2O$
Store at 4°C.

### Protein extraction

**RIPA Buffer**

| | Volume (ml) Or Weight (g) |
|---|---|
| **150 nM NaCl** | 1.5 ml |
| **1% Triton X100** | 0.5 ml |
| **0.1% SDS** | 0.5 ml |
| **10 mM Tris (PH 7.5)** | 0.5 ml |
| **1% Deoxycholate powder** | 0.5 g |

Adjust the volume to 50mL with distilled $H_2O$ and store at 4°C.

**7x protease inhibitor**

Dissolve 1 protease inhibitor tablet in 1.5 ml 1xPBS.
Aliquot and store at -20°C.

**RIPA solution (for 500 µl)**

| | Volume (µl) |
|---|---|
| **RIPA buffer** | 423 µl |
| **7x Protease inhibitor** | 71 µl |

Prepare on ice.
Make fresh before each use.

## SDS-PAGE reagents

**1.5M Tris pH 6.8 or pH 8.8**

Dissolve 60.5g Tris base in 300 ml $dH_2O$.
Adjust pH with concentrated HCl.
Fill up to 500 ml with $dH_2O$.
Store at 4°C.

**10% Sodium dodecyl sulphate (SDS)**

Dissolve 10g sodium dodecyl sulphate crystals in 80 ml $dH_2O$.
Adjust volume to 100 ml with $dH_2O$.
Store at room temperature.

**0.1% SDS**

Dissolve 0.05g sodium dodecyl sulphate in 40 ml $dH_2O$.
Adjust volume to 50 ml with $dH_2O$.
Store at room temperature.

**10% Ammonium persulfate (APS)**

Dissolve 0.1g APS in 1 ml $dH_2O$.
Store at 4°C for up to 2 weeks.

**30% acryl-bisacrylamide (50 ml)**

| | Weight (g) |
|---|---|
| **Acrylamide** | 29g |
| **N.N'-methylenebisacrylamide** | 1g |

Dissolve in 60 ml $dH_2O$, and heat the solution to 37°C to dissolve.
Adjust volume to 100 ml with $dH_2O$.
Filter through 0.45µM membrane.
Cover with foil and store at 4°C.

**10x SDS-PAGE running buffer (1 L)**

| | Weight (g) |
|---|---|
| **SDS** | 10g |
| **Tris** | 30.3g |
| **Glycine** | 144.1g |

Dissolve in 800 ml $dH_2O$.
Adjust volume to 1L with $dH_2O$.
Store at room temperature.

**1x SDS-PAGE running buffer**

1:10 dilution of 10x SDS-PAGE running buffer with $dH_2O$.
Store at room temperature.

**10x SDS-PAGE transfer buffer (1 L)**

| | Weight (g) |
|---|---|
| **Tris** | 38g |
| **Glycine** | 144g |

**1x SDS-PAGE transfer buffer**

| | Volume (ml) |
|---|---|
| **10X SDS-PAGE Transfer Buffer** | 100 ml |
| **Isopropanol** | 200 ml |
| **$dH_2O$** | 700 ml |

Make fresh and store at 4°C.

**1x Ponceau S staining solution (0.1% (w/v) Ponceau S in 5% (v/v) acetic acid)**

Dissolve 0.1g Ponceau S in 5 ml acetic acid
Adjust volume to 100 ml with $dH_2O$.
Cover with foil and store at room temperature.

**10 – 15% Resolving gel (7.5 ml)**

| | 10% gel Volume (ml) | 12% gel Volume (ml) | 15% gel Volume (ml) |
|---|---|---|---|
| **$dH_2O$** | 2.95 ml | 2.4 ml | 1.65 ml |
| **30% acryl-bisacrylamide mix** | 2.5 ml | 3 ml | 3.75 ml |
| **1.5m Tris pH 8.8** | 1.9 ml | 1.95 ml | 1.95 ml |
| **10% SDS** | 0.075 ml | 0.075 ml | 0.075 ml |
| **10% APS** | 0.075 ml | 0.075 ml | 0.075 ml |
| **tetramethylethylenediamine (TEMED)** | 0.003 ml | 0.003 ml | 0.003 ml |

Prepare and mix well.
Add the TEMED last.
Pour into a 1 mm glass plate and allow to set under an overlay of 0.1% SDS.

**5% Stacking gel (3 ml)**

| | Volume (ml) |
|---|---|
| **$dH_2O$** | 2.1 ml |
| **30% acryl-bisacrylamide mix** | 0.5 ml |
| **1.5m Tris pH 6.8** | 0.35 ml |
| **10% SDS** | 0.03 ml |
| **10% APS** | 0.03 ml |
| **tetramethylethylenediamine (TEMED)** | 0.003 ml |

Prepare and mix well.
Add the TEMED last.
Pour into a 1 mm glass plate, on top of the set resolving gel.
Add comb and allow to set.

**5x SDS loading dye (10 ml)**

| | Volume (ml)/ Weight (g) |
|---|---|
| **10% SDS** | 1 g |
| **0.04% Bromophenol blue** | 0.004 g |
| **2M Tris pH 6.8** | 1.25 ml |
| **100% Glycerol** | 3 ml |
| **β-mercaptoethanol** | 0.5 ml |

Dissolve the 10% SDS and 4% Bromophenol blue in 5.25 ml $dH_2O$.
Add the remaining components and mix.
Aliquot and store at room temperature.

## Western blotting

**10x Tris-buffered saline (TBS) (1 L)**

| | Weight (g) |
|---|---|
| **Tris** | 60.6 g |
| **NaCl** | 87.6 g |

Dissolve in 800 ml $dH_2O$.
Adjust pH to 6.8 with concentrated HCl.
Make up to 1 L with $dH_2O$, autoclave and store at 4°C.

**1x TBS**

1:10 dilution of 10x TBS with $dH_2O$.
Store at 4°C.

**1x TBS-Tween 20 (0.1%)**

Add 1 ml Tween-20 to 1x TBS (made up to 1L)
Mix well and store at 4°C.

**1x PBS-Tween 20 (0.1%)**

Add 1 ml Tween-20 to 1x PBS (made up to 1L)
Mix well and store at 4°C.

**5% fat-free milk in 1x TBS-Tween 20 (0.1%)**

Mix 41.7ml fresh fat-free milk with 58.3 ml 1x PBS/Tween-20(0.1%)
Store at 4$^{o}$C.

**5% BSA (w/v) in 1x TBS-Tween 20(0.1%)**

Dissolve 0.5 g BSA in 10 ml 1 x TBS/Tween-20(0.1%)
Store at 4$^{o}$C.

**Stripping buffer (100 ml)**

| | **VOLUME (ML)** |
|---|---|
| **β-mercaptoethanol** | 0.7 ml |
| **10% SDS** | 20 ml |
| **1.5m Tris-HCl pH 6.8** | 4.2 ml |
| **$dH_2O$** | 75.1 ml |

Mix well and store at room temperature.